Electronic Supplementary Material (ESI) for Polymer Chemistry.

SUPPLEMENTARY INFORMATION

Exploiting CH/π Interactions in Robust Supramolecular Adhesives

Taiki Yamate,[1]* Takayuki Fujiwara,[2] Toru Yamaguchi,[2] Hiroshi Suzuki,[1] Motohiro Akazome,[3]

[1]*Nippon Soda Co. Ltd., Chiba Research Center, 12-54 Goi-minamikaigan, Ichihara, Chiba 290-0045, Japan. E-mail: t.yamate@nippon-soda.co.jp*
[2]*Division of Computational Chemistry, Transition State Technology Co. Ltd., 2-16-1, Tokiwadai, Ube, Yamaguchi 755-8611, Japan.*
[3]*Department of Applied Chemistry and Biotechnology, Graduate School of Engineering, Chiba University, 1-33 Yayoicho, Inageku, Chiba 263-8522, Japan.*

The supplementary information includes:

1. Instrumentations.

^{1}H (500 MHz) and ^{13}C (125 MHz) NMR spectra were recorded on a JEOL ECP-500 spectrometer in chloroform-d_1 ($CDCl_3$) and *o*-dichlorobenzene-d_4, with tetramethylsilane as an internal standard (δ 0 ppm) for both nuclei. High-resolution mass spectra (HRMS) were recorded on a Bruker MicroTOF II mass spectrometer. Elemental analysis was carried out using a Perkin-Elmer PE2400II instrument. Fourier-transform infrared (FT/IR) spectroscopy was carried out using a JASCO FT/IR-6300 instrument. Attenuated total reflection (ATR) measurements were performed on the FT-IR instrument equipped with a germanium prism using single-reflection ATR accessories. Transmission measurements were performed using a fixed cell equipped with a KRS-5 aperture plate. Molecular weights were determined by gel permeation chromatography (GPC) using Waters 2695 system equipped with a refractive index detector and poly(methyl methacrylate) standards to calibrate the instrument. Differential scanning calorimetry (DSC) was performed on a TA Instruments DSC Q2000 machine. X-ray photoelectron spectroscopy (XPS) data were acquired on an ULVAC-PHI Quantera II instrument. X–ray diffraction (XRD) measurements were performed using a Rigaku Ultima IV diffractometer. Field-emission scanning electron microscopy (FE-SEM) was conducted using a JEOL JSM-7401F microscope. A cross sectional sample was made according to the following procedure. First, we cut into the sample with a cutter, and dipped it in liquid nitrogen. We then snapped the sample in two along the groove. Atomic force microscopy (AFM) measurements were carried out using a Hitachi High-Tech Science Corporation SPA400 microscope. Lap shear test was conducted on a SHIMADZU Universal/Tensile Testing Machine AGS-J equipped with a 5 kN load cell. A long-term humidity and heat test was carried out using a temperature and humidity chamber (Yamato Scientific Co. Ltd., IW242).

2. Synthesis and Characterization of **D1**, **D2** and **D3**.

- Synthesis of **D1**

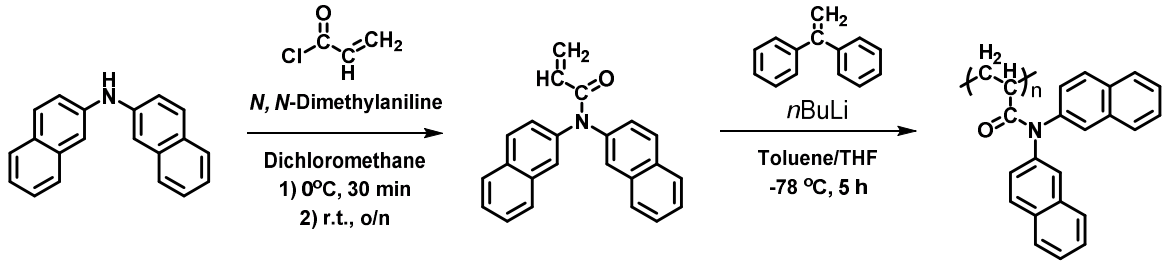

Monomer **D1** Polymer **D1**

Monomer **D1**.

2,2'-Dinaphthylamine (10.0 g, 37.1 mmol) and *N,N*-dimethylaniline (6.75 g, 55.7 mmol) were added to 200 mL THF in a round-bottom flask equipped with septum and stir bar. The mixture was cooled in ice bath for 30 min. Acryloyl chloride (4.03 g, 44.6 mmol) was added slowly to the flask through a syringe dropwise at 0 °C. The reaction was allowed to proceed under room temperature overnight. THF was removed by vacuum distillation, and the residue dissolved in ethyl acetate and washed with 1M HCl solution, $NaHCO_3$ solution and brine. The solution was dried over $MgSO_4$ and then concentrated to afford the crude product which was purified using column chromatograph on silica gel (silica gel 60, 63-200 mesh) with ethyl acetate:toluene (1/40 v/v) as the mobile phase. The solvent was removed and the product dried in vacuum to afford monomer **D1** (9.73 g, 30.1 mmol, 81% yield) as yellow oil.

^{1}H NMR (500 MHz, chloroform-d_1, TMS): δ/ppm = 5.64 (dd, J=1.9 Hz, 8.3 Hz,1H), 6.28 (dd, J=10.2 Hz, 6.6 Hz, 1H), 6.54 (dd, J=1.9 Hz, 14.9 Hz, 1H) , 7.37-7.59 (m, 6H), 7.67-7.91 (m, 8H). ^{13}C NMR (125 MHz, chloroform-d_1): δ/ppm = 125.7, 126.8, 127.8, 127.9, 128.8, 129.4, 130.0, 132.1, 133.6, 140.1, 166.3. HRMS–ESI (m/z): [M+Na$^+$] calcd for $C_{23}H_{17}N_1O_1$, 346.1202; found, 346.1200. Anal. Calcd for $C_{23}H_{17}N_1O_1$: C, 85.42; H, 5.30; N, 4.33. Found. C, 85.21; H, 5.50; N, 4.06. IR (cm^{-1}): 3079, 3057, 3031 (ν_{CH}; naphthalene ring), 1670 ($\nu_{C=O}$; amide).

Polymer **D1**.

Monomer **D1** (5.00 g, 15.5 mmol), 1,1-diphenylethylene (55.7 mg, 0.31 mmol), toluene 36 mL and THF 9 mL were added to a three-neck flask with a three-way stopcock. The reaction flask was sealed with a rubber septum and purged with nitrogen for 30 min. *n*BuLi (15wt% in Hexane) 0.10 mL was added slowly to the flask through a syringe dropwise at -78 °C. The reaction was allowed to proceed at -78 °C for 5 h and stopped by addition of a tiny amount of methanol. The obtained polymer was precipitated into a large amount of hexane and collected by centrifugation. The obtained polymer was dried overnight at 120 °C for in vacuo.

T_g (DSC): 212.11 °C. M_n and Đ (GPC): 23.1×10^3 Da and 1.21. IR (cm^{-1}): 3084, 3053, 3023 (ν_{CH}, naphthalene ring), 2920 (ν_{aCH}, methylene), 2876 (ν_{aCH}, methine), 1667 ($\nu_{C=O}$, amide).

- Synthesis of **D2**

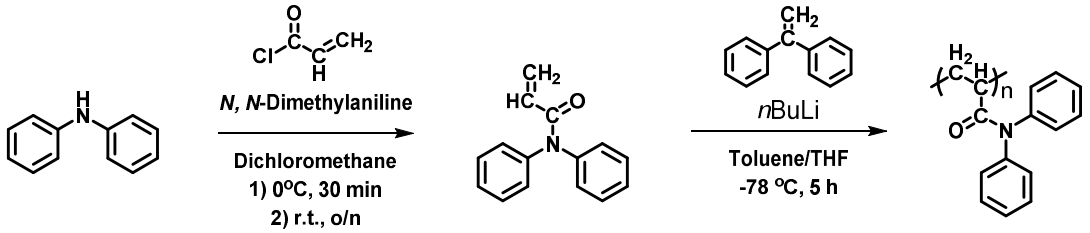

Monomer **D2** Polymer **D2**

Monomer **D2**.

Monomer **D2** was synthesized according to the reported procedure.[1] Diphenylamine (25.0 g, 148 mmol) and *N,N*-diphenylaniline (26.8 g, 222 mmol) were added to 270 mL dichloromethane (CH_2Cl_2)in a round-bottom flask equipped with septum and stir bar. The mixture was cooled in ice bath for 30 min. Acryloyl chloride (16.7 g, 185 mmol) was added slowly to the flask through a syringe dropwise at 0 °C. The reaction was allowed to proceed under room temperature overnight. CH_2Cl_2 was removed by vacuum distillation, and the residue dissolved in ethyl acetate and washed with 1M HCl solution, $NaHCO_3$ solution and brine. The solution was dried over $MgSO_4$ and then concentrated to afford the crude product which was recrystallized from Toluene/hexane to afford monomer **D2** (20.1 g, 90.1 mmol, 61% yield) as a white solid.

^{1}H NMR (500 MHz, chloroform-d_1, TMS): δ/ppm = 5.62 (dd, J=1.9 Hz, 8.6 Hz,1H), 6.19 (dd, J=10.3 Hz, 6.5 Hz, 1H), 6.47 (dd, J=1.9 Hz, 14.9 Hz, 1H) , 7.21-7.40 (m, 10H). ^{13}C NMR (125 MHz, chloroform-d_1): δ/ppm = 127.2, 128.4, 129.3, 129.7, 142.6, 165.8. HRMS–ESI (m/z): [M+Na$^+$] calcd for $C_{15}H_{13}N_1O_1$, 246.0880; found, 246.0891. IR (cm^{-1}): 3095, 3059, 3030 (ν_{CH}; benzene ring), 1663 ($\nu_{C=O}$; amide).

Polymer **D2**.

Monomer **D2** (5.00 g, 22.4 mmol), 1,1-diphenylethylene (40.0 mg, 0.22 mmol), toluene 16 mL and THF 4 mL were added to a three-neck flask with a three-way stopcock. The reaction flask was sealed with a rubber septum and purged with nitrogen for 30 min. *n*BuLi (15wt% in Hexane) 0.14 mL was added slowly to the flask through a syringe dropwise at -78 °C. The reaction was allowed to proceed at -78 °C for 5 h and stopped by addition of a tiny amount of methanol. The obtained polymer was precipitated into a large amount of hexane and collected by centrifugation. The obtained polymer was dried overnight at 120 °C for in vacuo.

T_g (DSC): 215.25 °C. M_n and Đ (GPC): 22.8×10^3 Da and 1.27. IR (cm^{-1}): 3096, 3064, 3033 (ν_{CH}, benzene ring), 2934 (ν_{aCH}, methylene), 2865 (ν_{aCH}, methine), 1669 ($\nu_{C=O}$, amide).

- Synthesis of **D3**

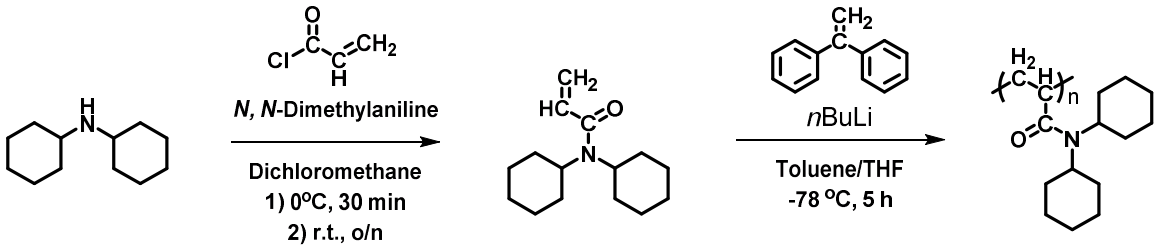

Monomer **D3** Polymer **D3**

Monomer **D3**.

Monomer **D3** was synthesized according to the reported procedure.[2] Dicyclohexylamine (25.0 g, 138 mmol) and *N,N*-diphenylaniline (20.1 g, 165 mmol) were added to 200 mL dichloromethane (CH_2Cl_2)in a round-bottom flask equipped with septum and stir bar. The mixture was cooled in ice bath for 30 min. Acryloyl chloride (15.0 g, 165 mmol) was added slowly to the flask through a syringe dropwise at 0 °C. The reaction was allowed to proceed under room temperature overnight. CH_2Cl_2 was removed by vacuum distillation, and the residue dissolved in ethyl acetate and washed with 1M HCl solution, $NaHCO_3$ solution and brine. The solution was dried over $MgSO_4$ and then concentrated to afford the crude product which was recrystallized from Toluene/hexane to afford monomer **D3** (25.0 g, 106 mmol, 77% yield) as a white solid.

^{1}H NMR (500 MHz, chloroform-d_1, TMS): δ/ppm = 6.55 (dd, J=7.8 Hz, 12.1 Hz,1H), 6.17 (dd, J=17.6 Hz, 2.2 Hz, 1H), 5.56 (dd, J=10.9 Hz, 2.3 Hz, 1H) , 3.09-3.61 (broad, 2H), 2.01-2.49 (broad, 2H), 1.39-1.88 (broad, 12H), 1.01-1.37 (broad, 6H). ^{13}C NMR (125 MHz, chloroform-d_1): δ/ppm = 166.5, 131.1, 125.7, 57.6, 55.8, 31.8, 30.2, 26.6, 26.2, 25.4. HRMS–ESI (m/z): [M+Na^+] calcd for $C_{15}H_{25}N_1O_1$, 258.1828; found, 258.1816. IR (cm^{-1}): 2937, 2857 (ν_{CH}; methylene), 1640 ($\nu_{C=C}$; vinyl), 1613 ($\nu_{C=O}$; amide).

Polymer **D3**.

Monomer **D3** (10.0 g, 42.5 mmol), 1,1-diphenylethylene (77.0 mg, 0.42 mmol), toluene 72 mL and THF 18 mL were added to a three-neck flask with a three-way stopcock. The reaction flask was sealed with a rubber septum and purged with nitrogen for 30 min. *n*BuLi (15wt% in Hexane) 0.27 mL was added slowly to the flask through a syringe dropwise at -78 °C. The reaction was allowed to proceed at -78 °C for 5 h and stopped by addition of a tiny amount of methanol. The obtained polymer was precipitated into a large amount of hexane and collected by centrifugation. The obtained polymer was dried overnight at 120 °C for in vacuo.

T_g (DSC): 264.94 °C. M_n and Đ (GPC): 22.1×10^3 Da and 1.22. IR (cm^{-1}): 2928, 2849 (ν_{CH}, methylene), 1630 ($\nu_{C=O}$, amide).

- NMR Spectroscopy

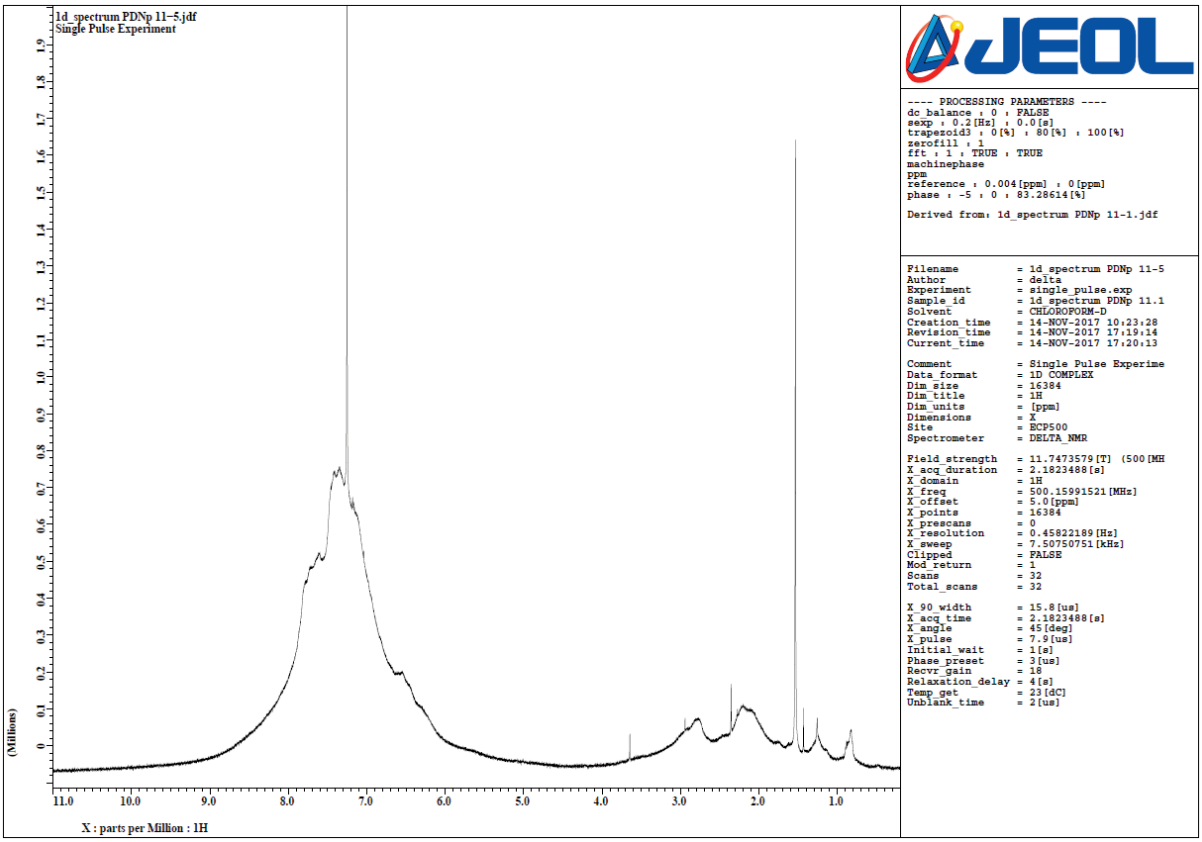

Figure S1 | ^{1}H NMR spectrum (500 MHz, r.t., Chloroform-d_1) of polymer **D1**.

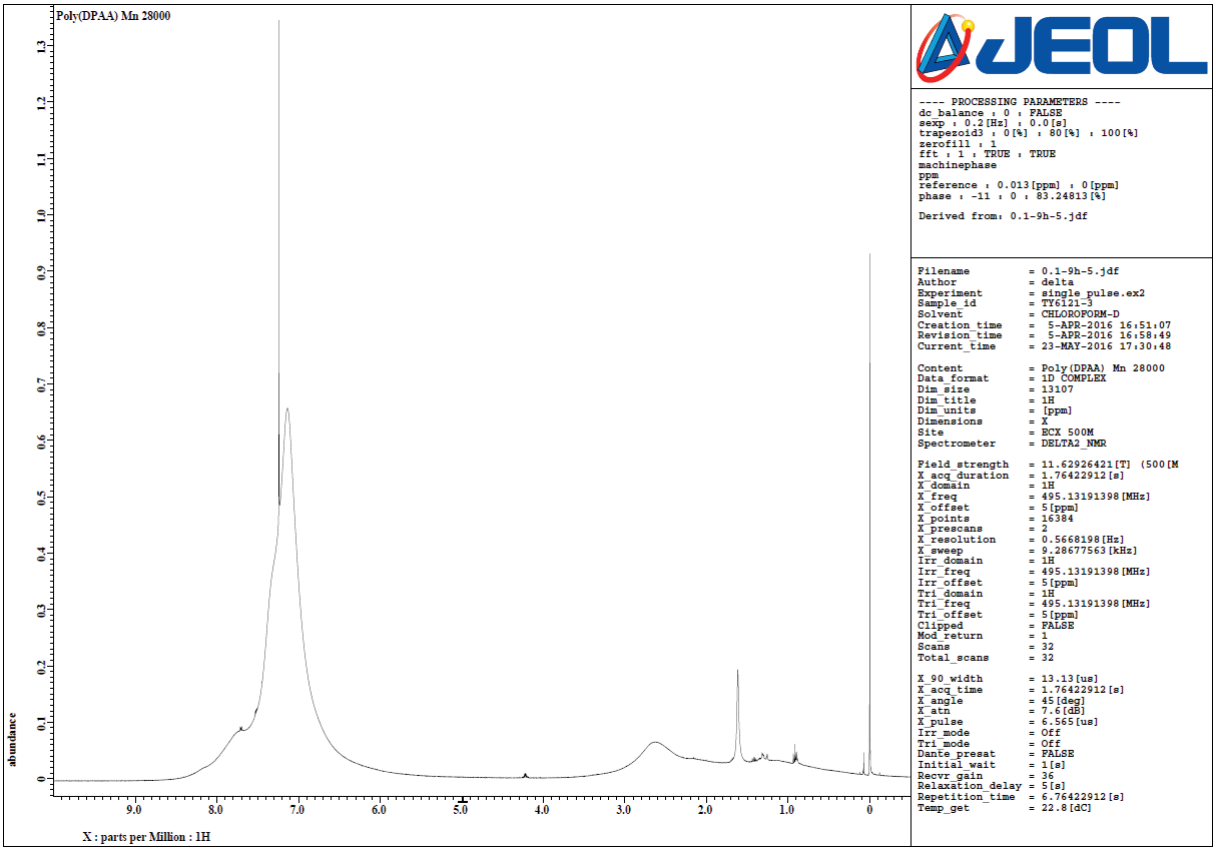

Figure S2 | ^{1}H NMR spectrum (500 MHz, r.t., Chloroform-d_1) of polymer **D2**.

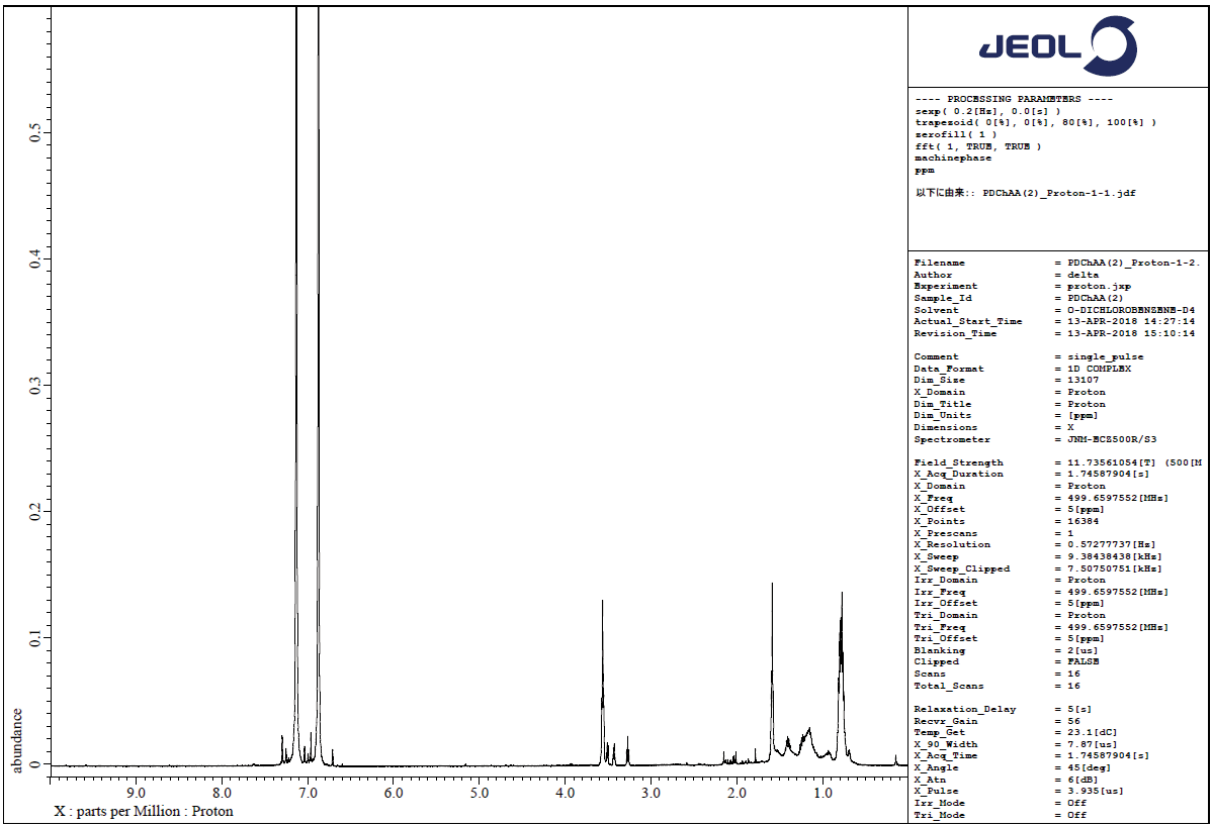

Figure S3 | ^{1}H NMR spectrum (500 MHz, r.t., *o*-dichlorobenzene-d_4) of polymer **D3**.

- Differential scanning calorimetry (DSC)

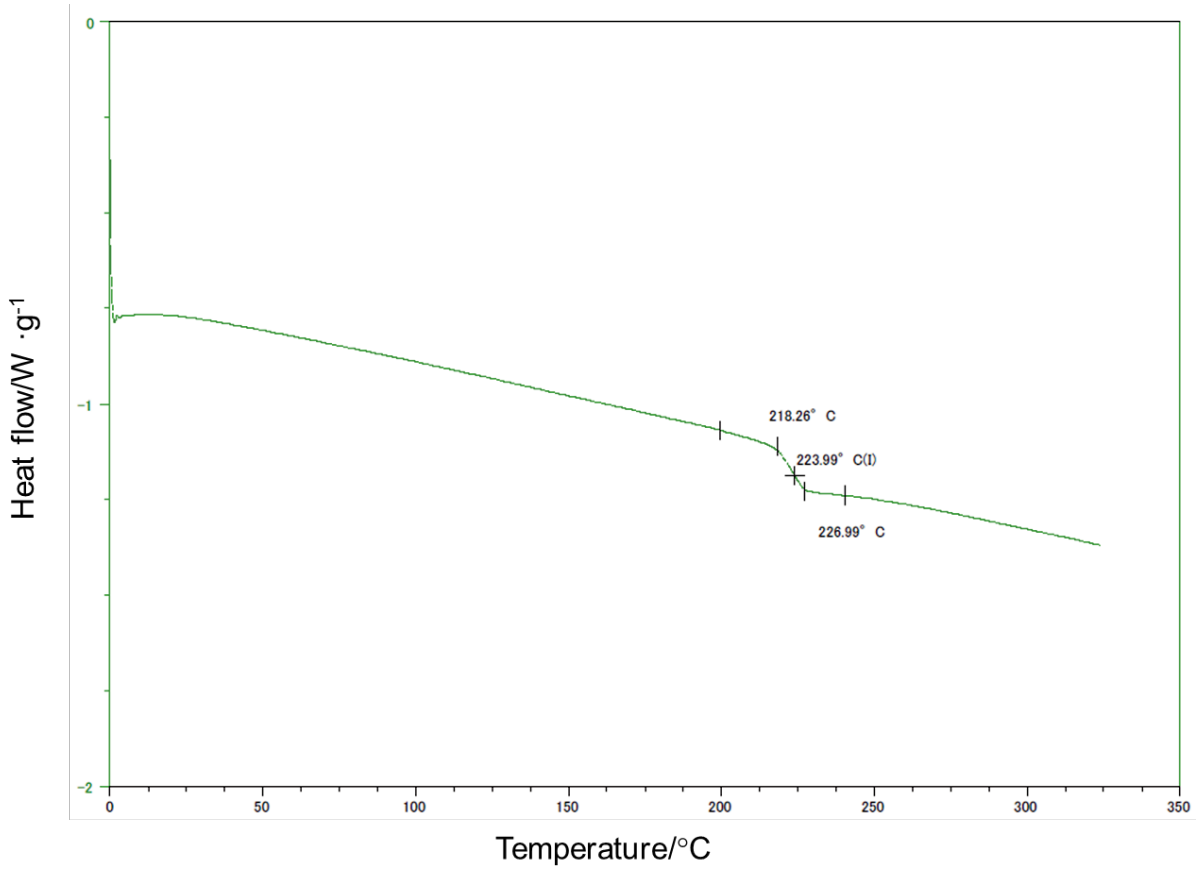

Figure S4 | DSC thermogram of polymer **D1**.

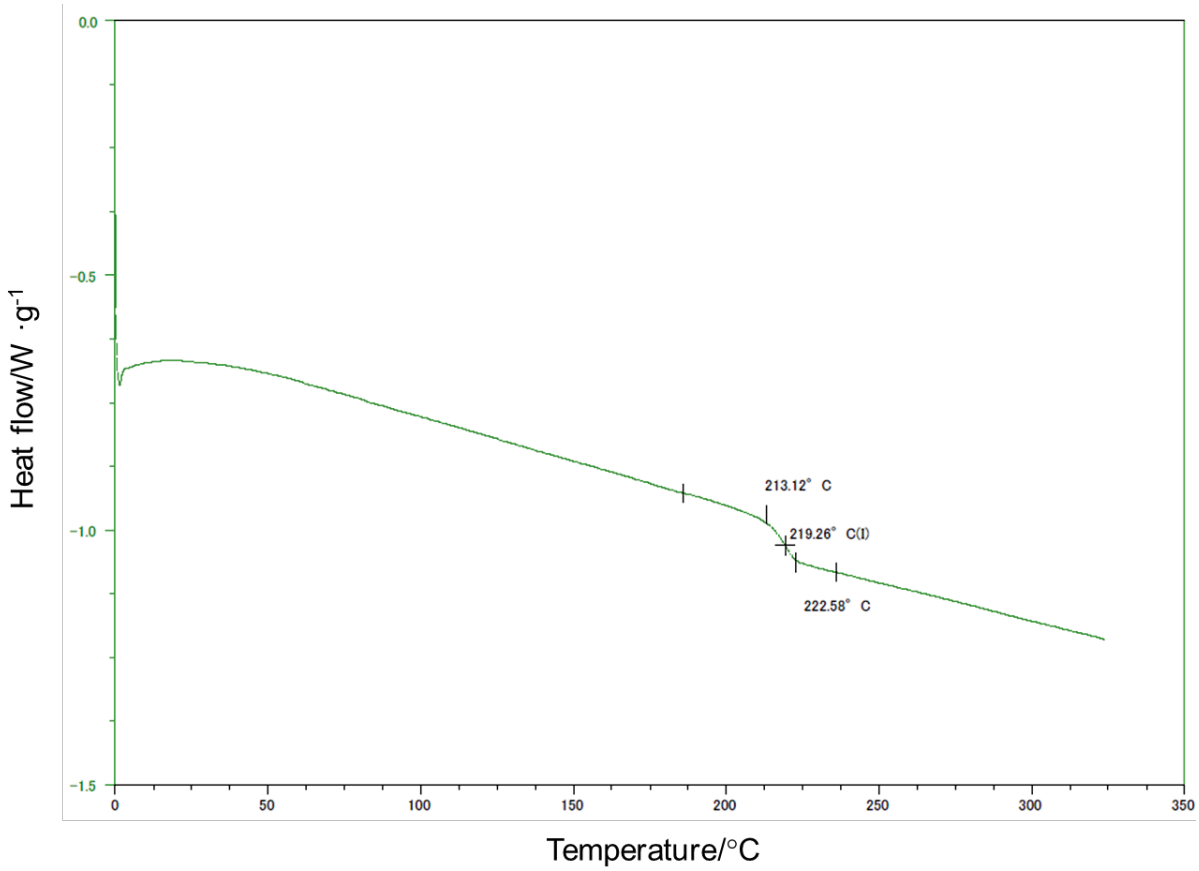

Figure S5 | DSC thermogram of polymer **D2**.

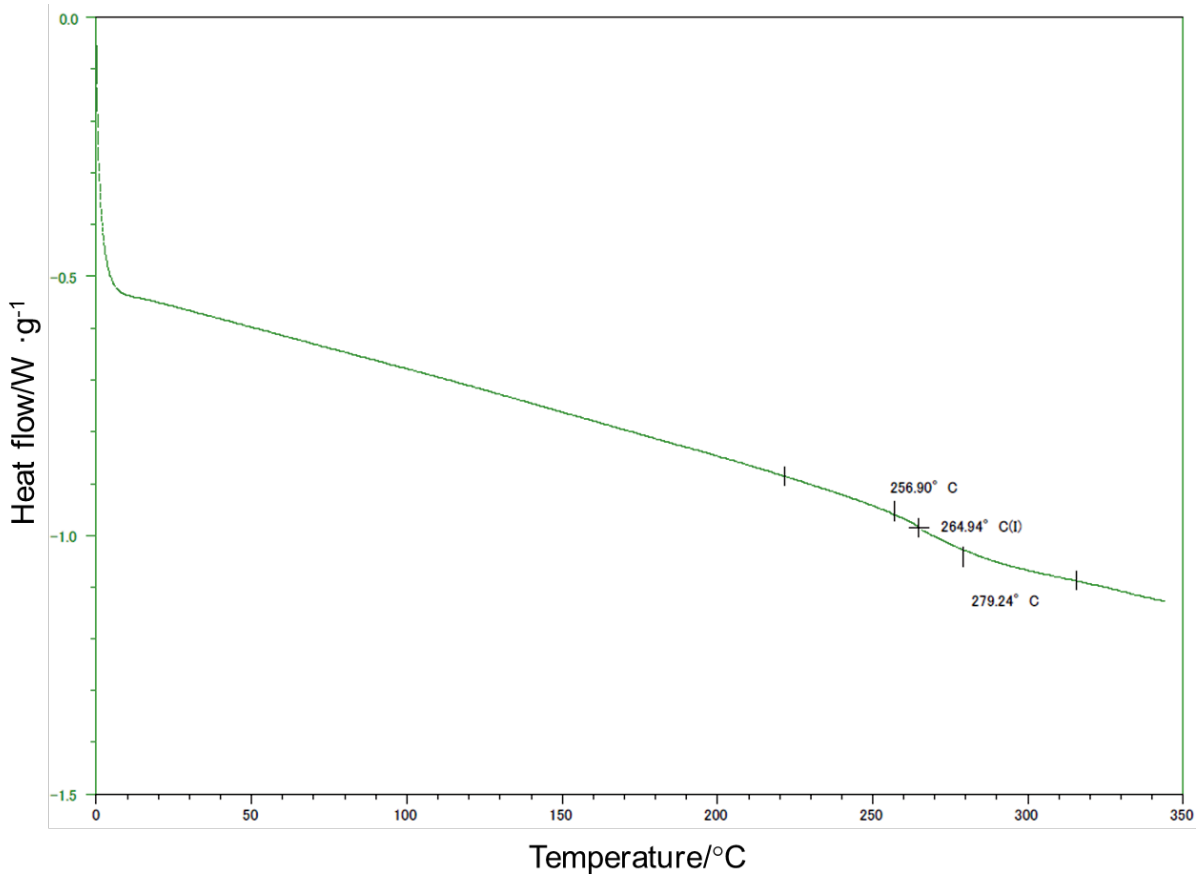

Figure S6 | DSC thermogram of polymer **D3**.

- Attenuated Total Reflection (ATR) FT-IR

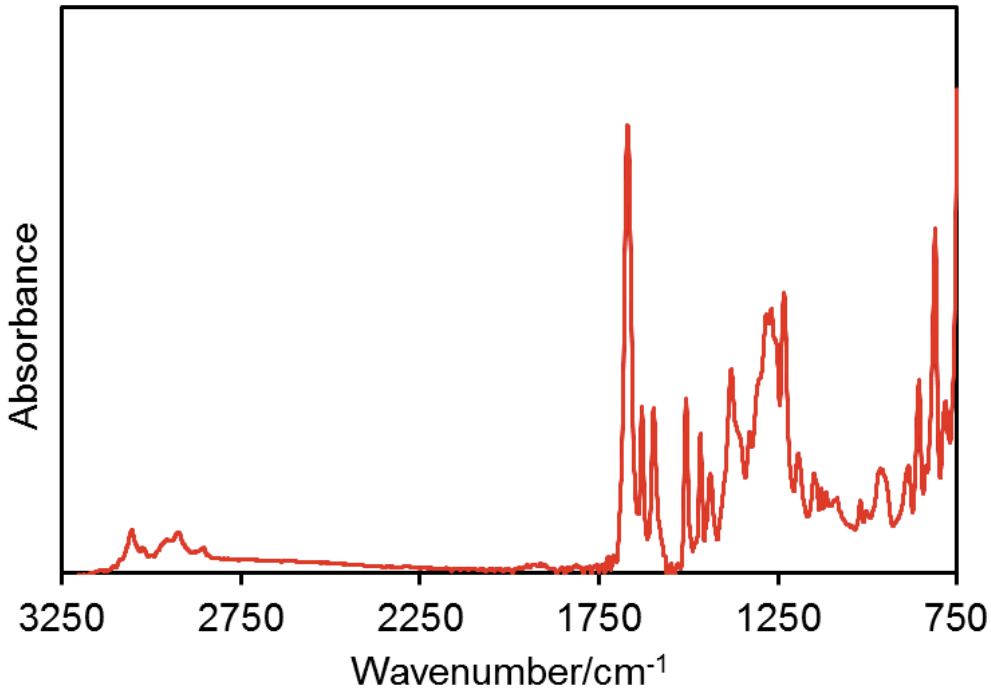

Figure S7 | FT-IR (ATR) spectrum of polymer **D1**.

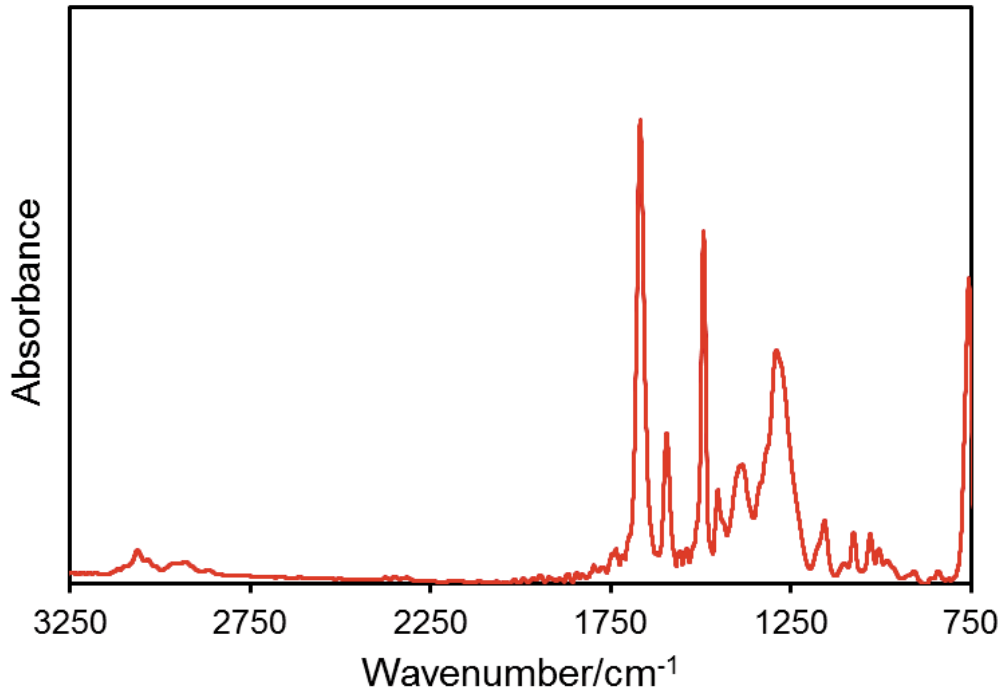

Figure S8 | FT-IR (ATR) spectrum of polymer **D2**.

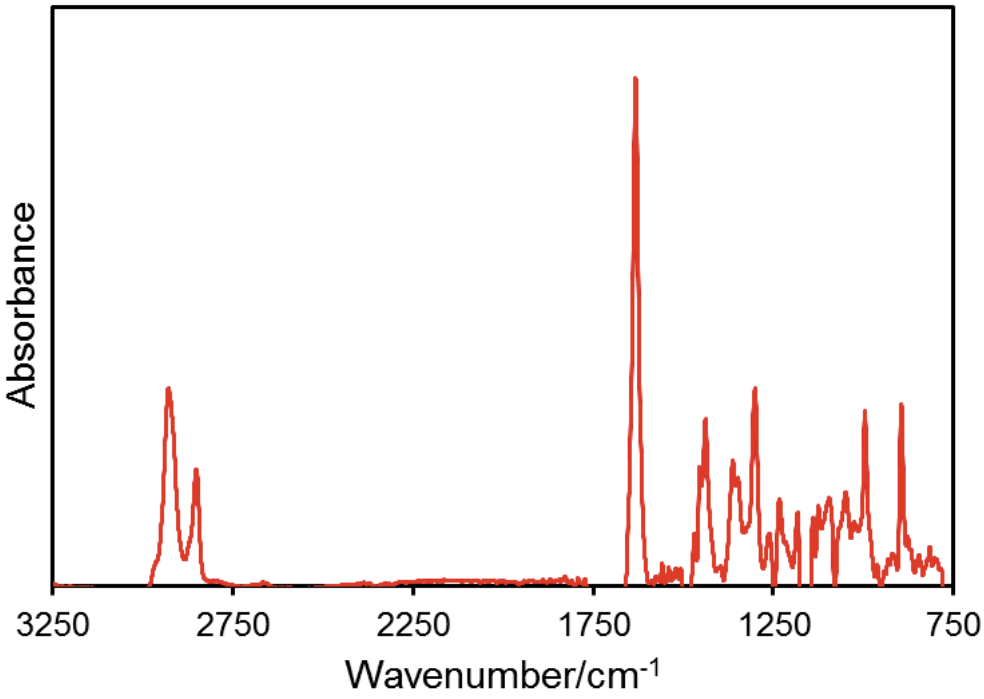

Figure S9 | FT-IR (ATR) spectrum of polymer **D3**.

3. Characterization of π acceptor substrates.

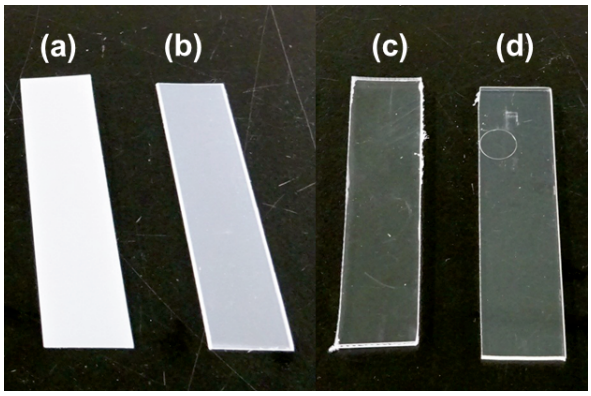

Figure S10 | Photograph of (a) **A1** (PE), (b) **A2** (PP), (c) **A3** (PMP) and **A4** (COP).

- ATR-FT-IR

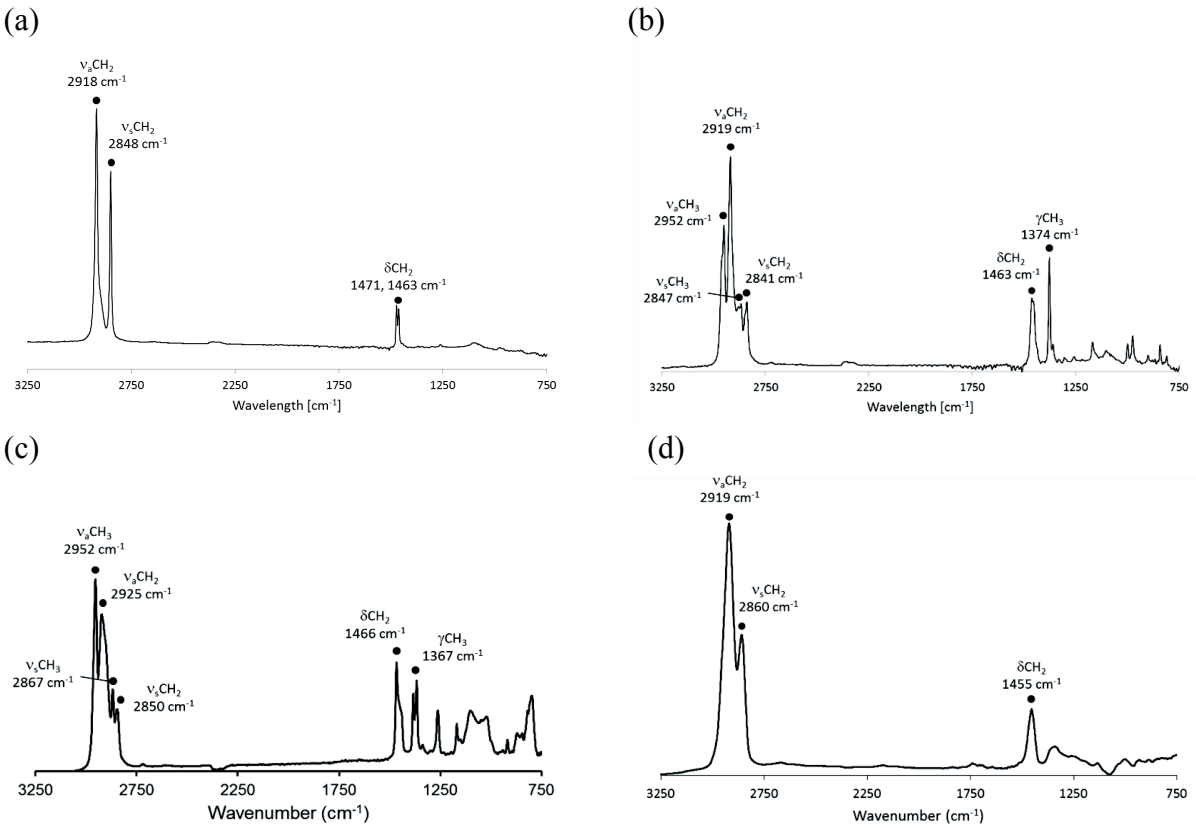

Figure S11 | ATR-FT-IR spectrum of (a) **A1**, (b) **A2**, (c) **A3** and (d) **A4**.

- X-ray Photoelectron Spectroscopy (XPS)

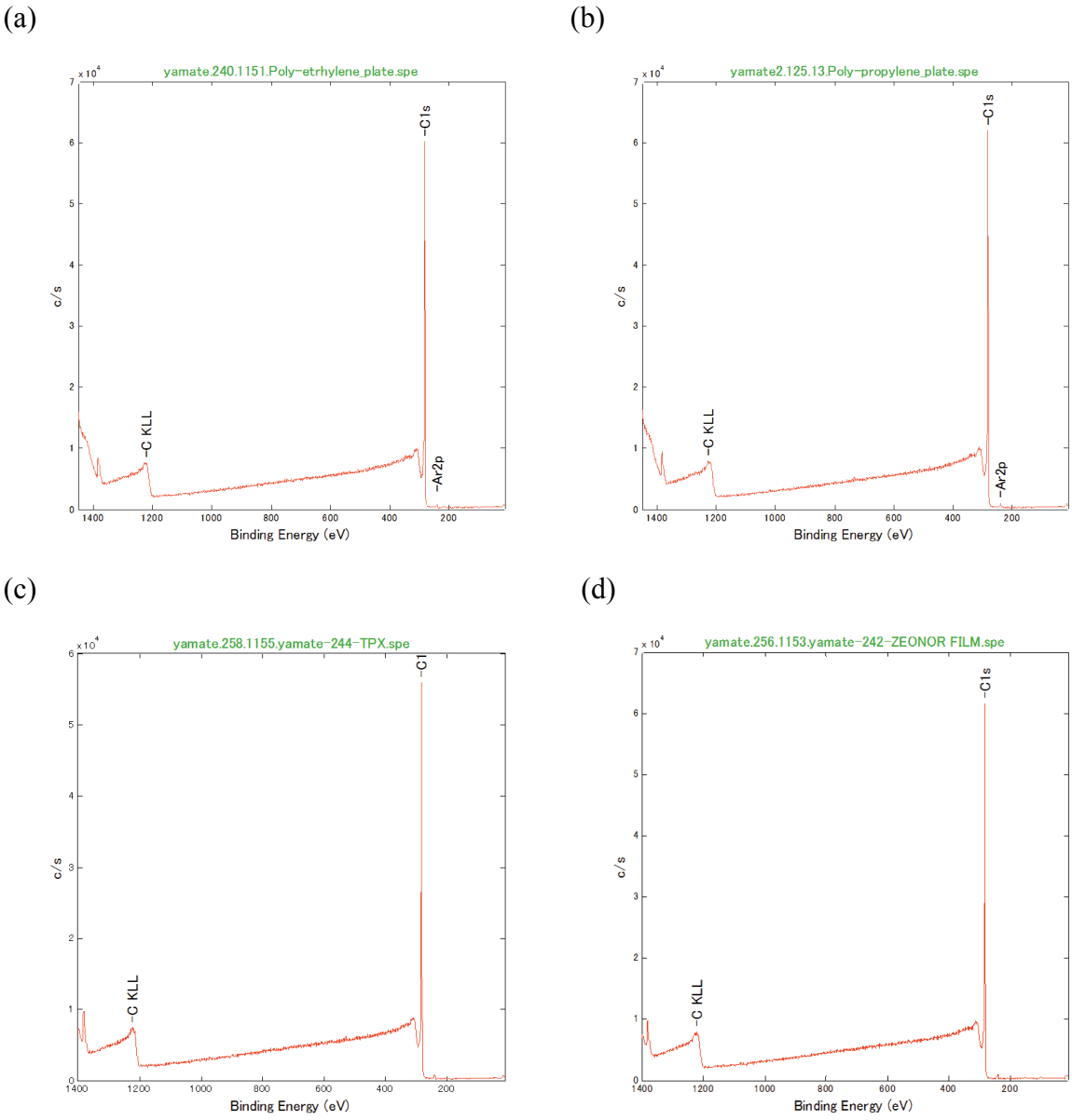

Figure S12 | XPS survey spectra of (a) **A1**, (b) **A2**, (c) **A3** and (d) **A4**.

- Atomic Force Microscope (AFM)

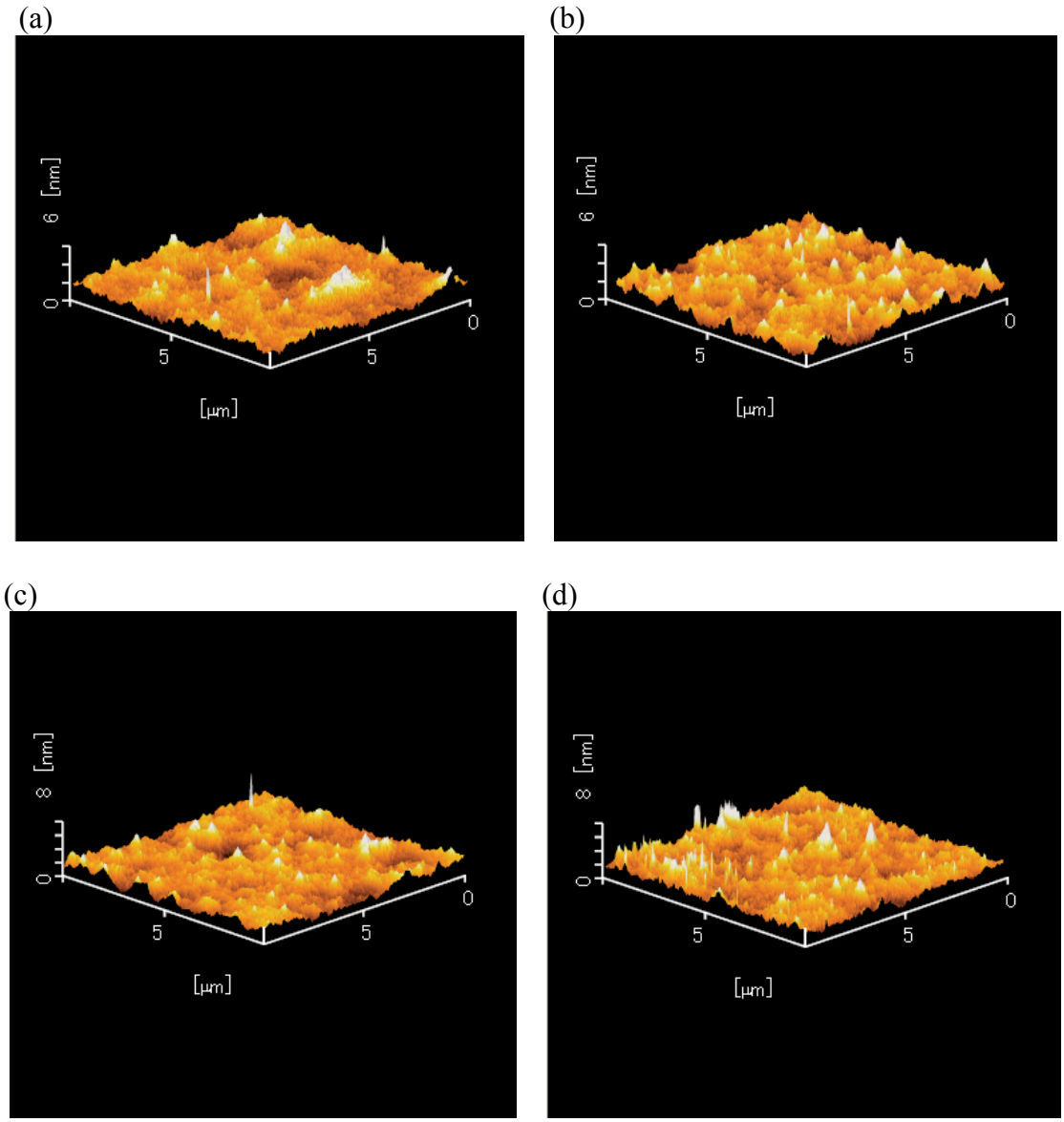

Figure S13 | AFM image of the (a) **A1**, (b) **A2**, (c) **A3** and (d) **A4**.
Root-mean-square (RMS) roughness value is 0.559 nm for **A1**, 0.589 nm for **A2**, 0.486 nm for **A3** and 0.520 nm for **A4**.

- X-Ray Diffraction (XRD)

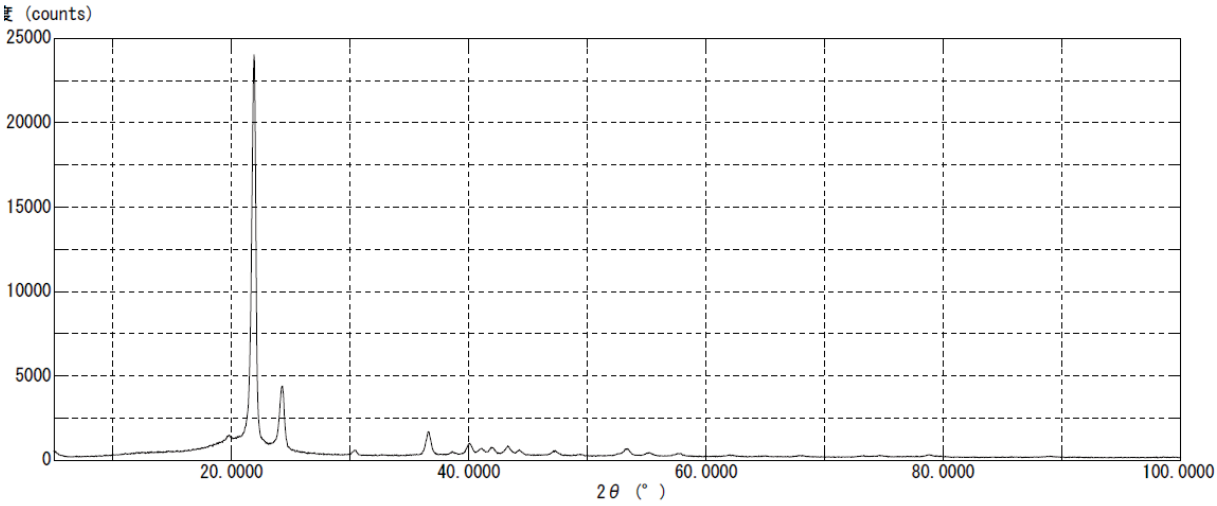

Figure S14 | XRD pattern of **A1**.

4. Preparation of samples for adhesion testing.

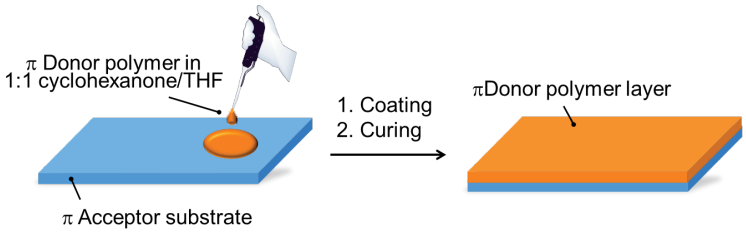

Figure S15 | Schematic diagram showing the adhesion of π donor and π acceptor polymers.

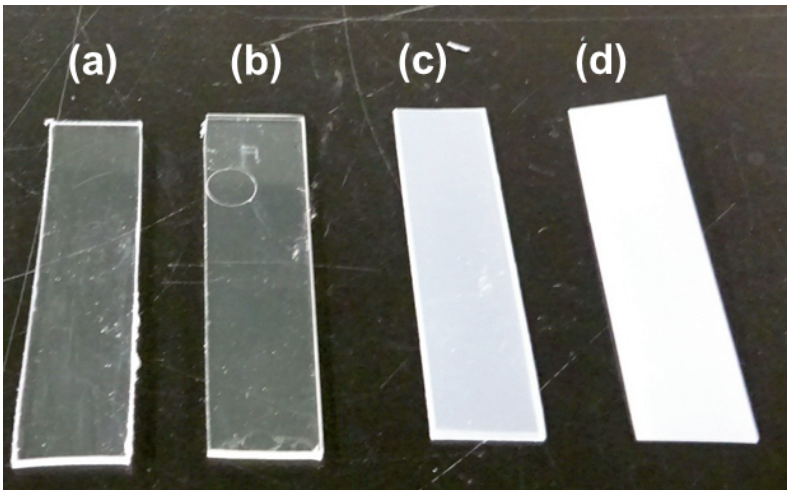

Figure S16 | Photograph of samples fabricated polymer **D1** layer on (a) **A4**, (b) **A3**, (c) **A2** and (d) **A1**.

- ATR-FT-IR

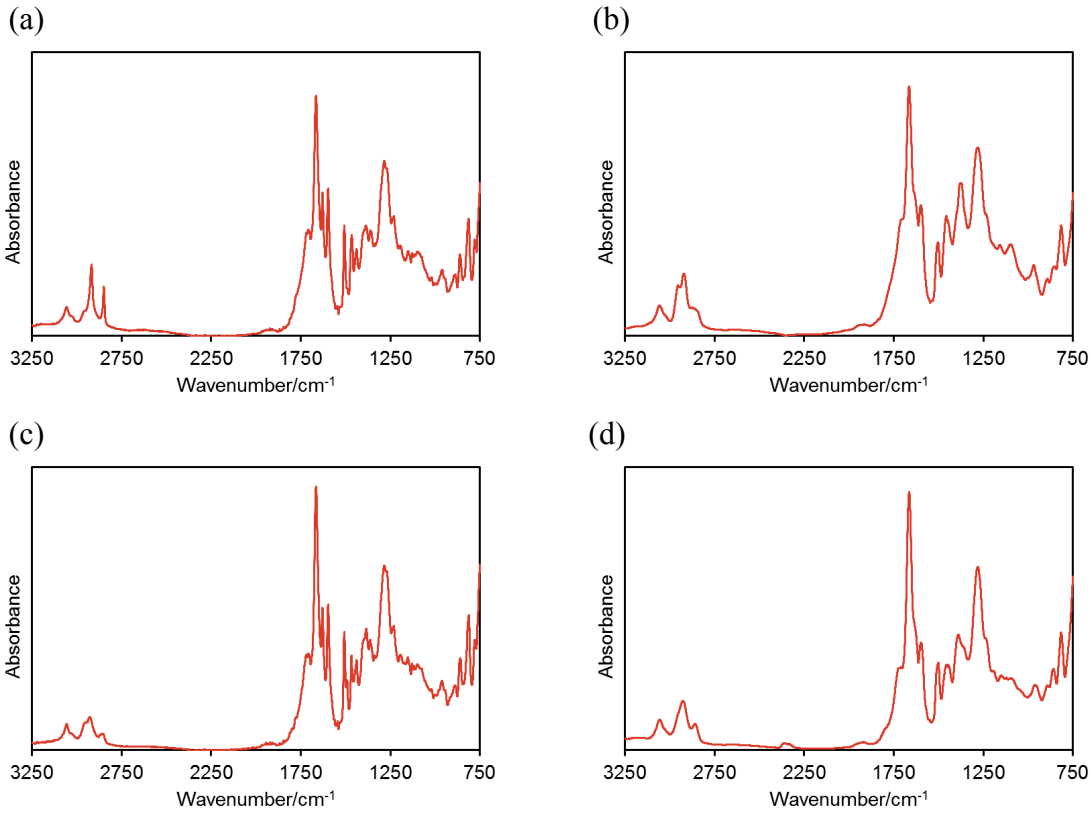

Figure S17 | FT-IR (ATR) spectrum of **D1** layers on (a) **A1**, (b) **A2**, (c) **A3** and (d) **A4**.

- XPS

(a)

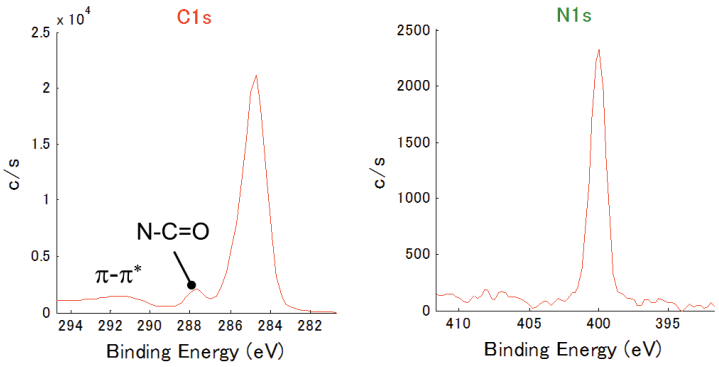

(b)

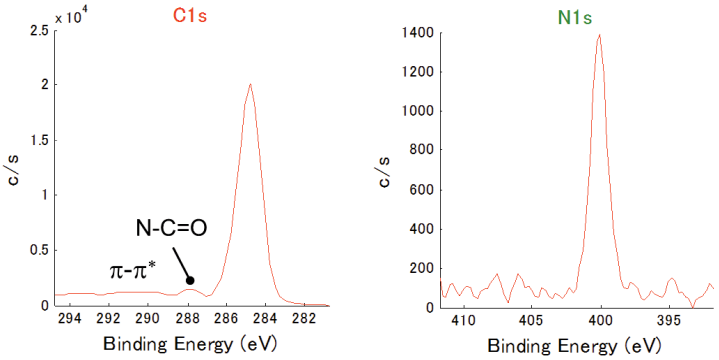

(c)

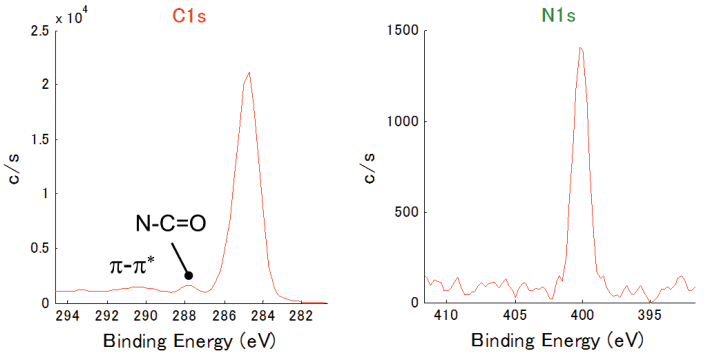

(d)

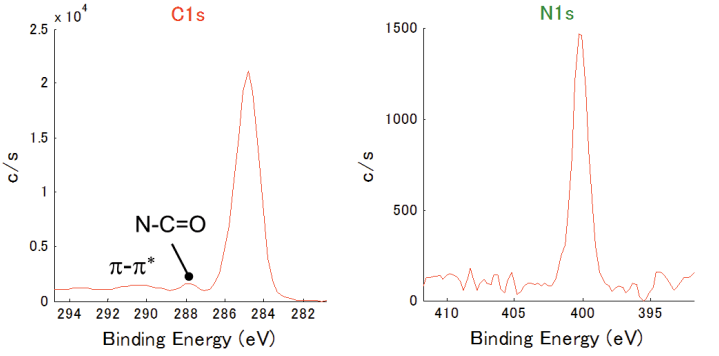

Figure S18 | The C1s and N1s peaks in the XPS spectrum of **D1** layers on (a) **A1**, (b) **A2**, (c) **A3** and (d) **A4**.

- Field Emission Scanning Electron Microscopy (FE-SEM)

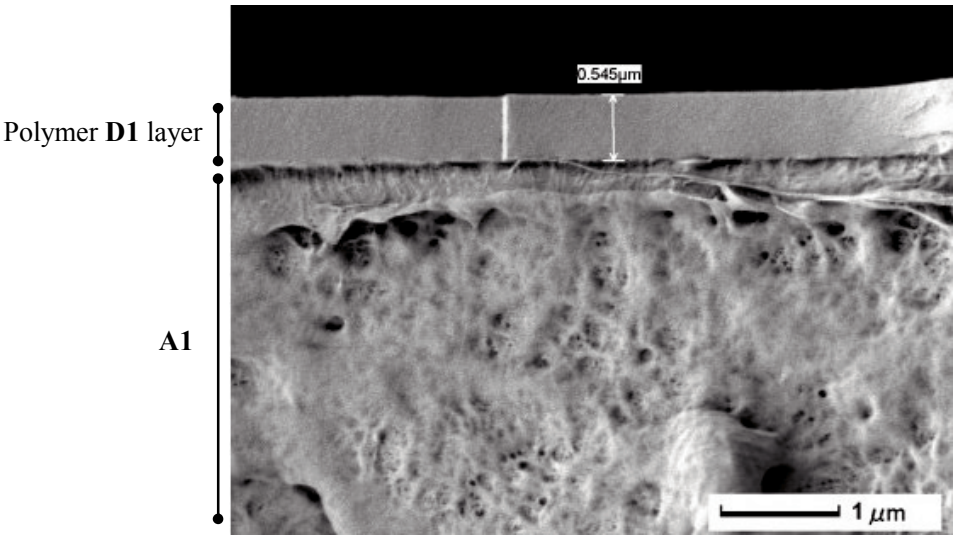

Figure S19 | FE-SEM image of polymer **D1** layer on **A1** substrate. Thickness of polymer **D1** layer is 545 nm.

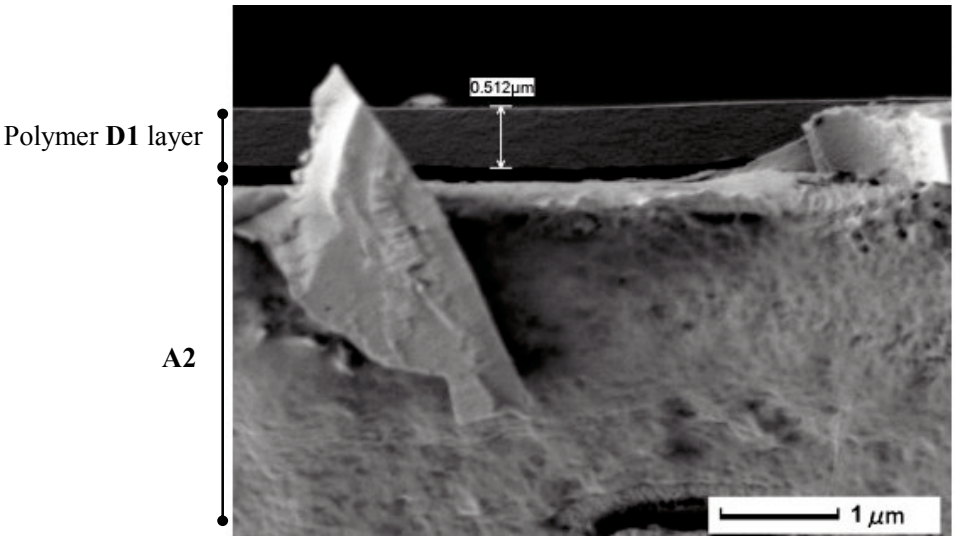

Figure S20 | FE-SEM image of polymer **D1** layer on **A2** substrate. Thickness of polymer **D1** layer is 512 nm.

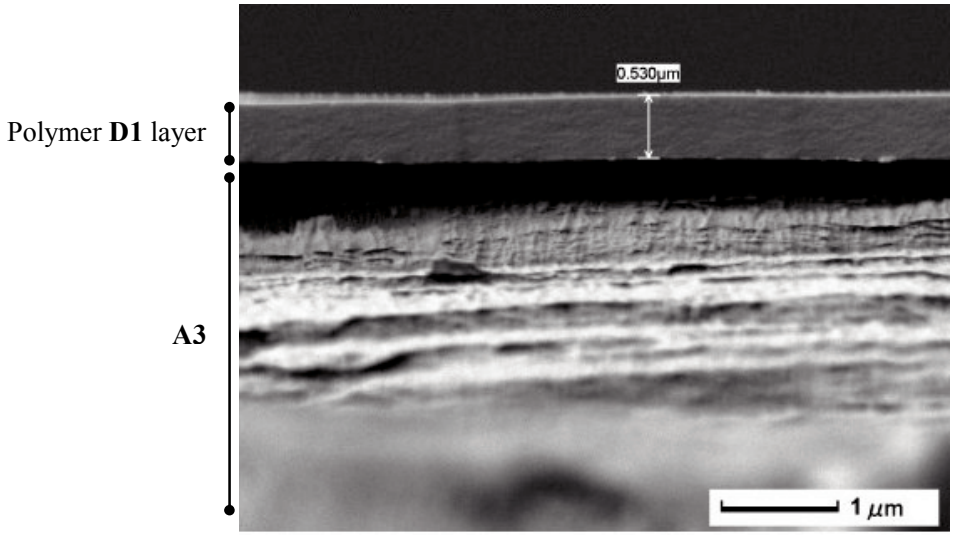

Figure S21 | FE-SEM image of polymer **D1** layer on **A3** substrate. Thickness of polymer **D1** layer is 530 nm.

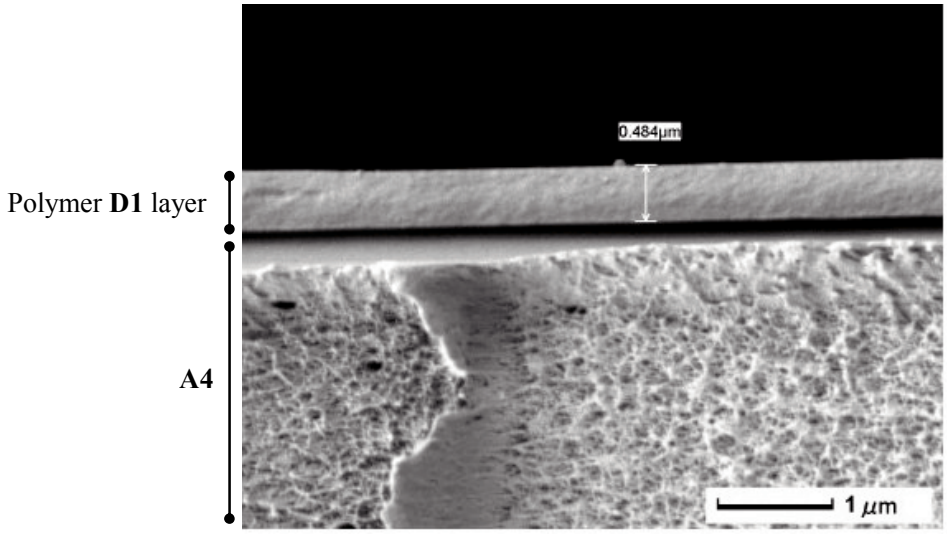

Figure S22 | FE-SEM image of polymer **D1** layer on **A4** substrate. Thickness of polymer **D1** layer is 484 nm.

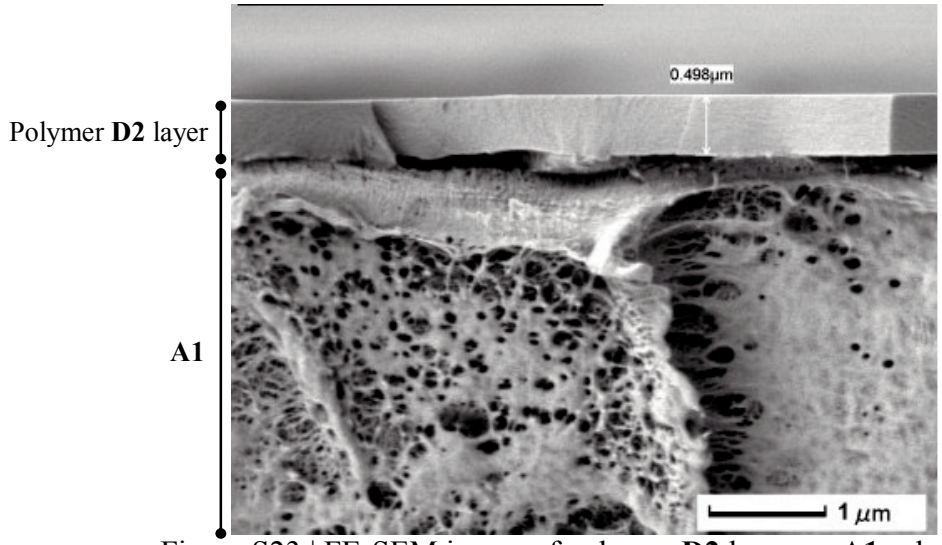

Figure S23 | FE-SEM image of polymer **D2** layer on **A1** substrate. Thickness of polymer **D2** layer is 498 nm.

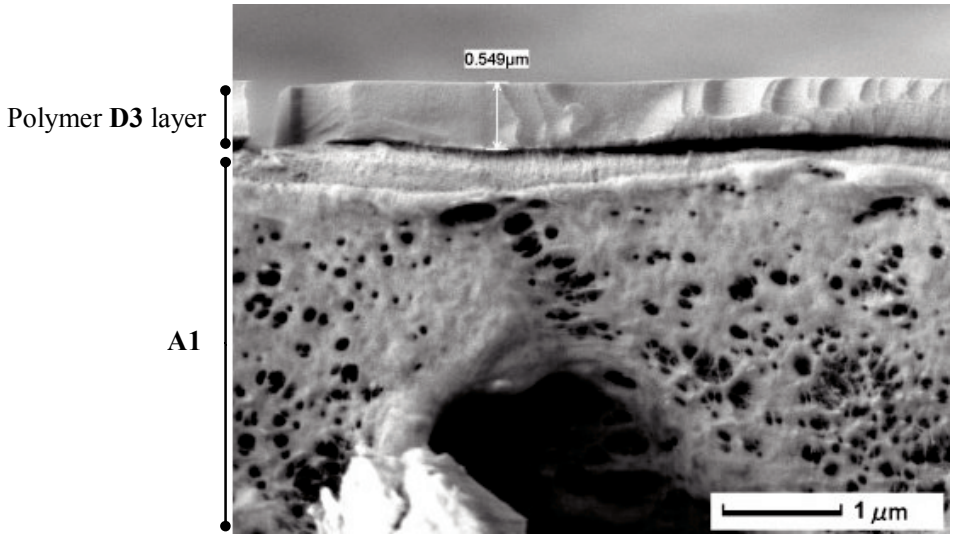

Figure S24 | FE-SEM image of polymer **D3** layer on **A1** substrate. Thickness of polymer **D3** layer is 549 nm.

5. Lap-shear test.

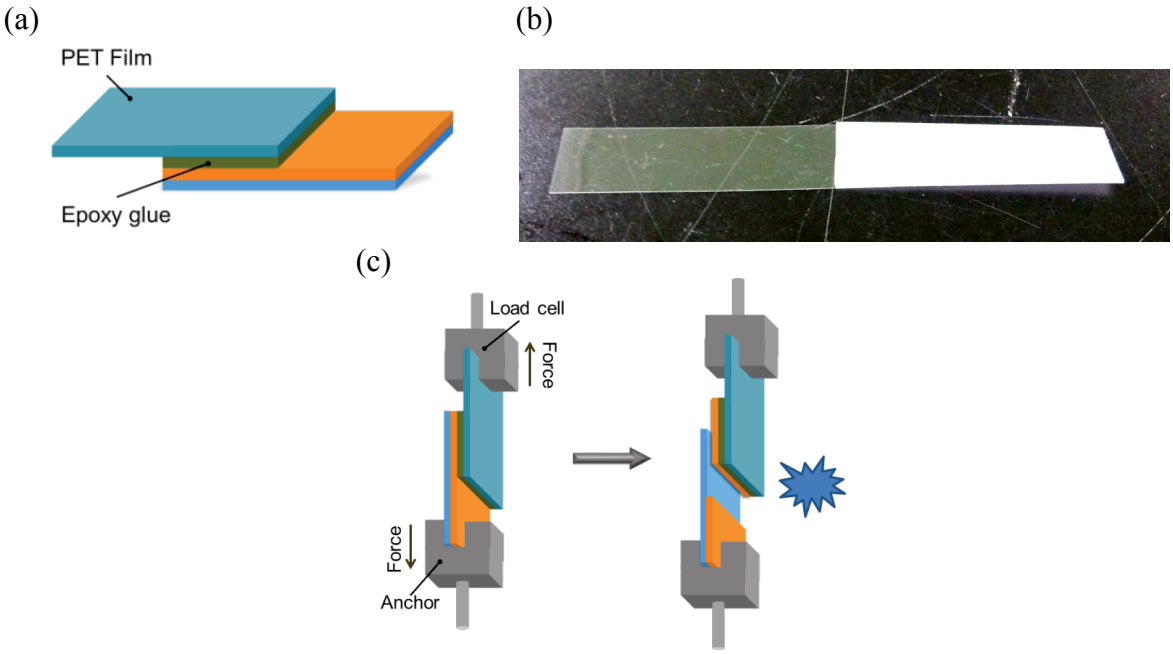

Figure S25 | (a) Schematic diagram of a lap-shear test sample, (b) photograph of lap-shear test samples, (c) schematic diagram of a loaded lap-shear test sample.

- ATR-FT-IR

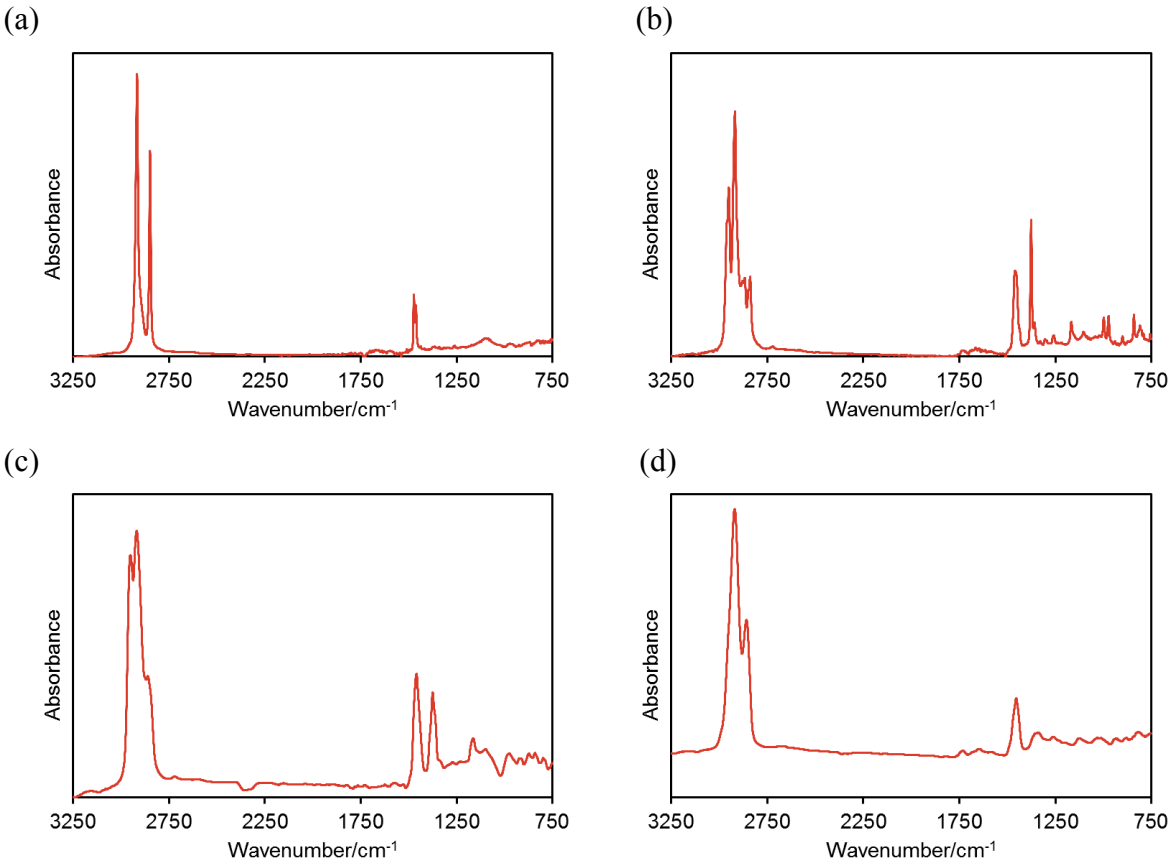

Figure S26 | FT-IR (ATR) spectrum of (a) **A1**, (b) **A2**, (c) **A3** and (d) **A4** after lap-shear test of polymer **D1** layer and π-acceptor polymers.

- XPS

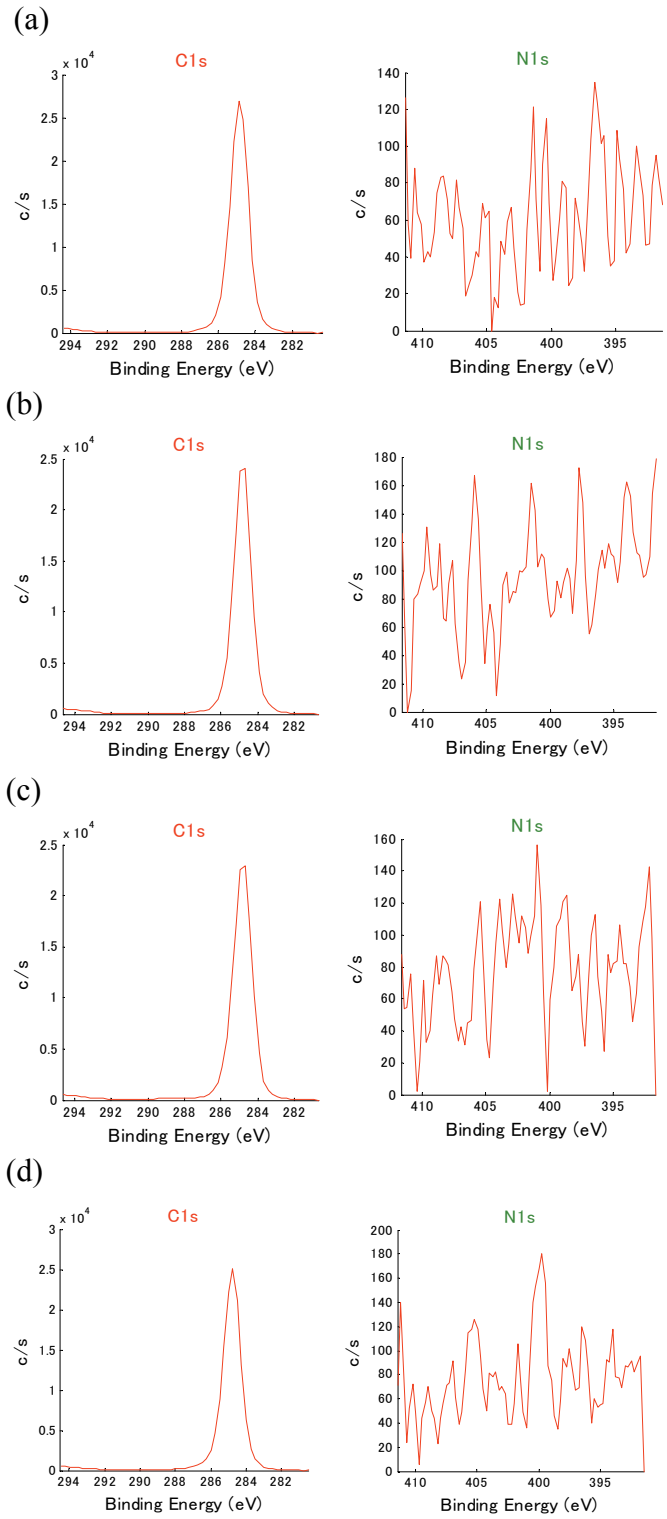

Figure S27 | C1s and N1s peaks in the XPS spectrum of (a) **A1**, (b) **A2**, (c) **A3** and (d) **A4** after lap-shear test of polymer **D1** and π-acceptor polymers.

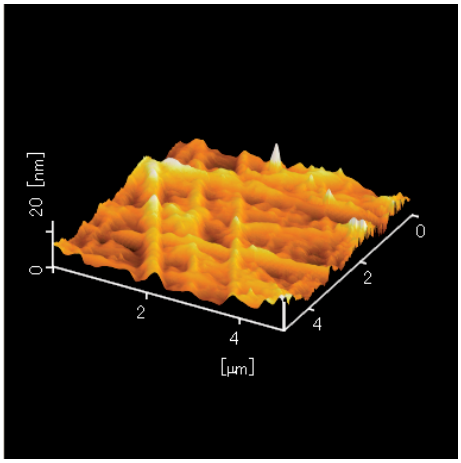

Figure S28 | AFM image of the **A1** substrate after lap-shear test of polymer **D1** and **A1** substrate. Root-mean-square (RMS) roughness value is 2.3 nm.

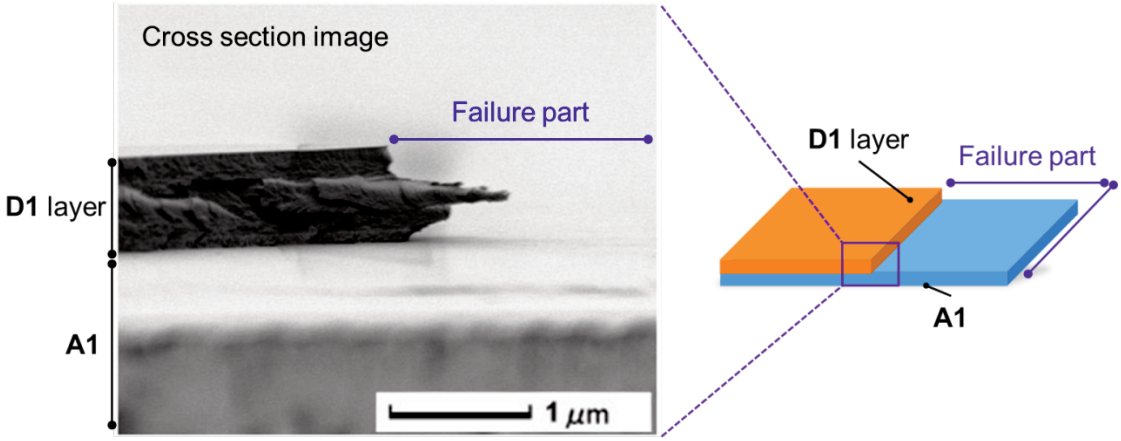

Figure S29 | FE-SEM cross section image of the failure point of sample after lap-shear testing of polymer **D1** and **A1** substrate.

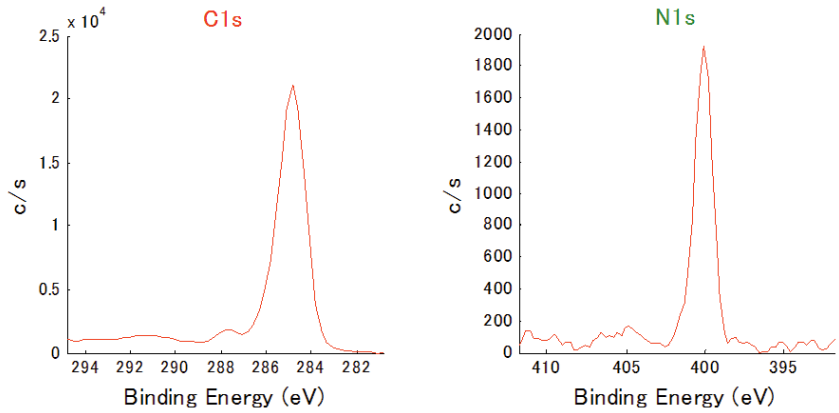

Figure S30 | The C 1s and N 1s peaks in the XPS spectrum of the failure point of the **D1** surface after lap-shear testing of polymer **D1** and **A1** substrate.

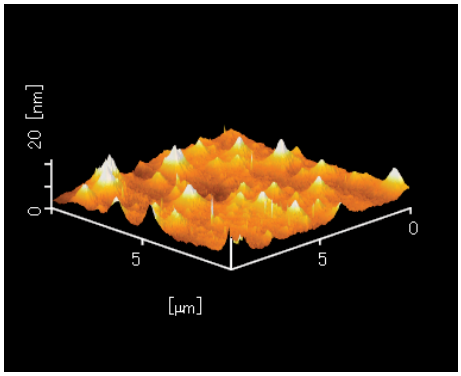

Figure S31 | AFM image of the failure point of the **D1** surface after lap-shear testing of polymer **D1** and **A1** substrate. RMS roughness value is 1.924 nm.

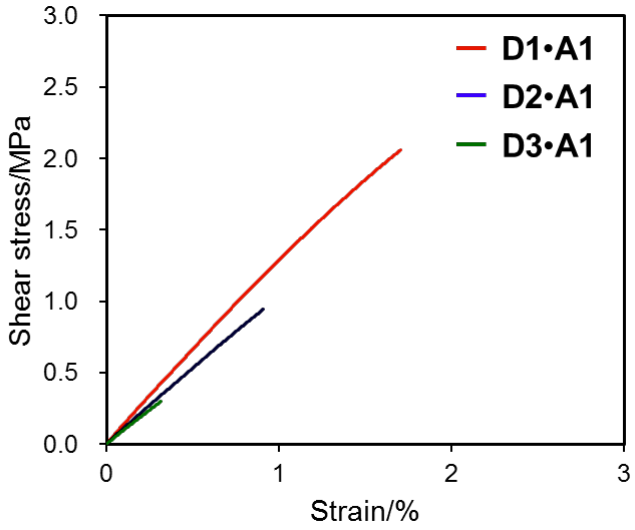

Figure S32 | Tensile stress−strain diagrams: **D1•A1**, **D2•A1** and **D3•A1**.

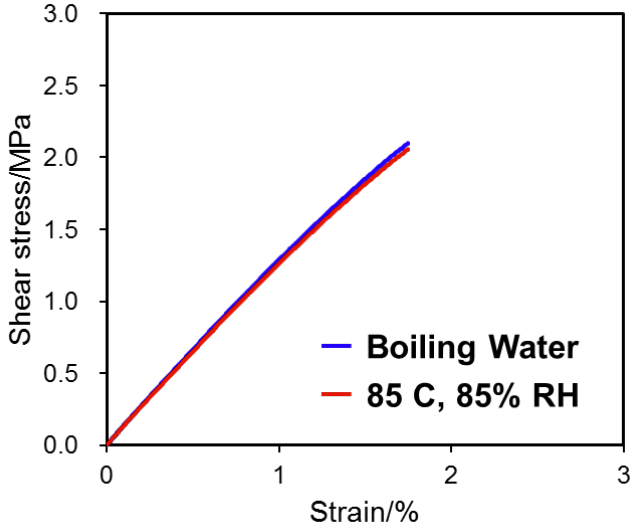

Figure S33 | Tensile stress−strain diagrams: **D1•A1** soaked in boiling water for 5 h and exposed to constant temperature and humidity (85 °C, 85% RH) for 30 d.

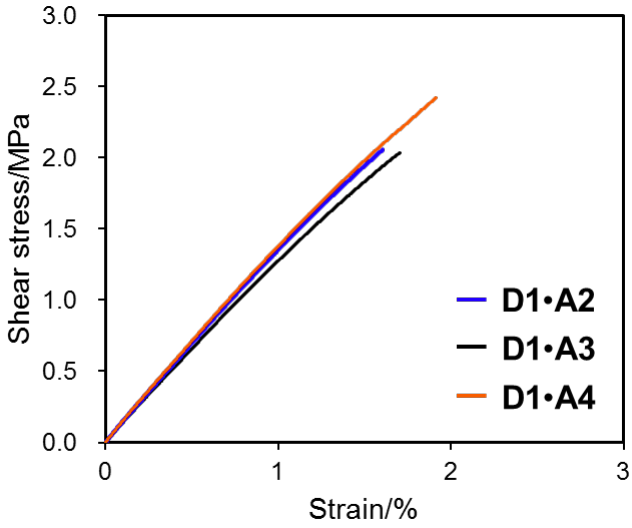

Figure S34 | Tensile stress−strain diagrams: **D1•A2**, **D1•A3** and **D1•A4**.

6. Tacticity of polymer **D1**.

Polymer **D1** were converted to poly(acrylic acid) by refluxing in methanol containing sulfuric acid overnight. The poly(acrylic acid) were methylated with trimethylsilyldiazomethane to poly(methyl acrylate) (PMA). This obtained PMA were collected by centrifugation, repeatedly washed with methanol, and dried in vacuo at 60 ºC. The tacticity of polymer **D1** was determined from the ^{1}H NMR spectra of the PMA derived from polymer **D1**.

Table S1 | Tacticity of polymer **D1**.

Run	*m*-diad/*r*-diad	Tacticity
Polymer **D1**	76/24	Isotactic

7. Computational details.

- Method

Density functional theory (DFT) calculations were performed using the 64-bit version of Gaussian 09 on a Linux cluster with 36-core Intel XEON processors (2.3 GHz) and 16 GB RAM per processor. The level of theory for all calculations was B3LYP/6-31G(d). The calculated IR spectra are presented by assigning a Lorentzian band shape with a half-width of 1 cm^{-1} to each fundamental vibration. The frequencies were scaled by a factor of 0.96 for better comparison with the experimental data. For some calculations, the modredundant option was used to fix several internal coordinates. The calculations were performed using the gauche and trans conformational isomers of **D1** (Figs. S29a, b). Figure S29c shows the DFT-calculated IR spectrum of **D1** in the wavenumber range between 1000 and 1200 cm^{-1}.

Computational analysis began with an initial geometry allocation to **D1**. We developed a dedicated program for generating Z-matrices for three-dimensional polymer structures, utilizing polymer tacticity ratios determined by ^{1}H NMR spectroscopy (Table S1) to build a sequence of meso or racemo monomer units with the exclusion of arbitrariness. Structures of **D1** were built using this program for 100 monomer units, with tacticities randomly arranged based on the observed tacticity ratios, utilizing Mersenne Twister to generate random numbers.[3]

The abovementioned initial geometry was optimized using molecular mechanics (MM) calculations at the UFF level of theory at 0 K in the gas phase.[4] The Gaussian 09 series of programs was used for all optimizations. UFF generally provides good results for organic molecules and was adopted due to practical CPU time considerations for 100 monomer units. [5] We investigated the pattern of trans and gauche backbone conformations in a stable structure of **D1** (Fig. 2c) by manually counting the dihedral angles of C–C bonds in the polymer main chain.

In order to simulate adhesive processes on the **A1** surface, molecular dynamics (MD) calculation was performed using the LAMMPS series of programs (2016 version).[6] Initial cell structure included **A1** surface and **D1** optimized by MM calculations. The centre of gravity of **D1** was set 10 Å away from the **A1** surface under two-dimensional periodic boundary conditions. The **A1** surface was fixed, exhibiting lattice constants of a = 0.740 nm, b = 0.493 nm, c = 0.254 nm, $\alpha = \beta = \gamma = 90°$ (Fig. S14). Simulation was performed with NPT ensembles at atmospheric pressure and room temperature, with each unit cell represented by a 240-Å-wide, 160-Å-high, and 160-Å-deep cuboid. The GAFF[7] force field was adopted and the particle mesh Ewald (PME) method[8] was used for calculating the Coulomb force, while the Nose-Hoover method[9,10] was used for temperature control, and the Berendsen method[11] was used for pressure control. The sampling time was set at 200 ps, with the first 5 ps reserved for the heating processes to ensure that the average system temperature was around 298.15 K. Equilibrium calculation was performed 50 ps after commencement, when fluctuations confirmed the equilibration of energy. Radial distribution functions (RDFs) were computed based on trajectories simulated by MD calculation.

- Computational analysis of backbone conformation of **D1**

Table S2 | The trans and gauche conformation ratio of the polymer backbone in a stable structure of **D1** obtained by the MM method.

Run	trans	gauche
Polymer **D1**	64	36

- Calculation of IR spectrum

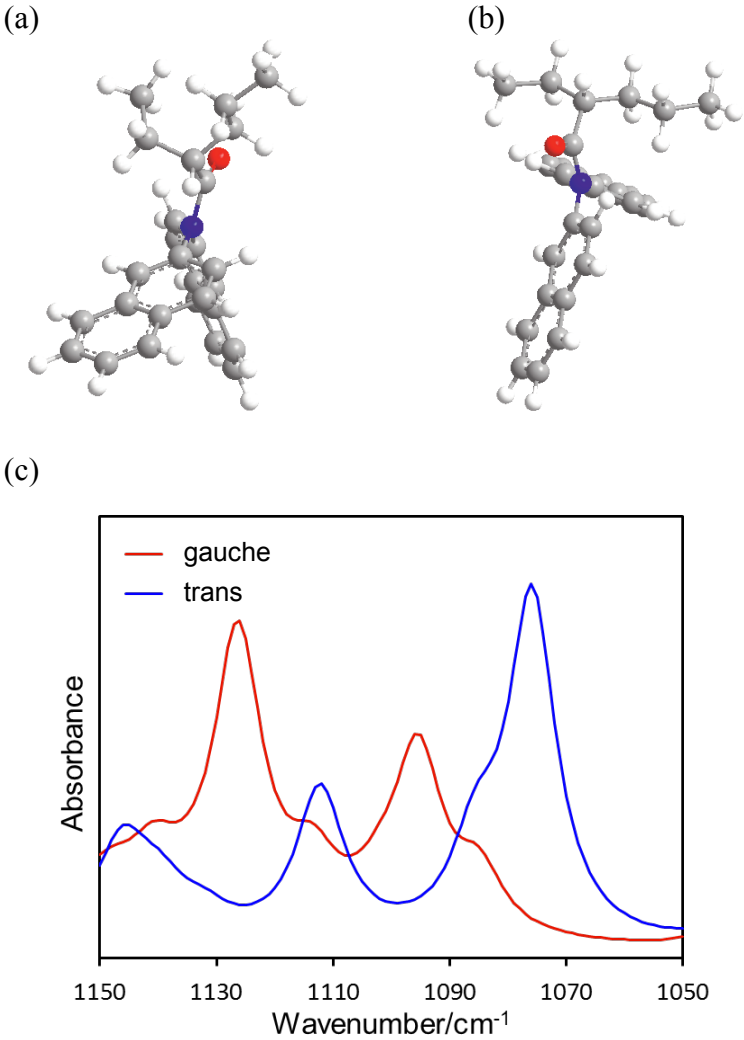

Figure S35 | 3D models representing schematically the (a) gauche and (b) trans conformational isomers of **D1**. (c) IR spectra in the range between 1050 and 1150 cm^{-1} obtained from DFT calculation.

8. Interfacial analysis between π-donor polymers and **A1** by experimental study.

The macroscopic **D1**–**A1** interface was experimentally analysed using IR spectroscopy. First, we investigated the structure of **D1** on the **A1** surface by attenuated total reflection (ATR) FT-IR. The sample had a thinner **D1** layer, with a thickness of around 30 nm (Fig. S36), to gain highly intensive absorption of the interface. In addition, to negate some absorption peaks originating from **A1** in the range of 1000 to 1200 cm^{-1}, we used the difference absorption spectrum (Fig. S37) which was obtained by subtracting the spectrum of **A1** from that of the prepared sample. **D1** showed a strong absorption peak at 1075 cm^{-1} and a smaller peak at 1129 cm^{-1}, attributed to the trans and gauche conformations, respectively. This result showed that the **D1** had formed extended-polymer-chain structures on the **A1** surface.

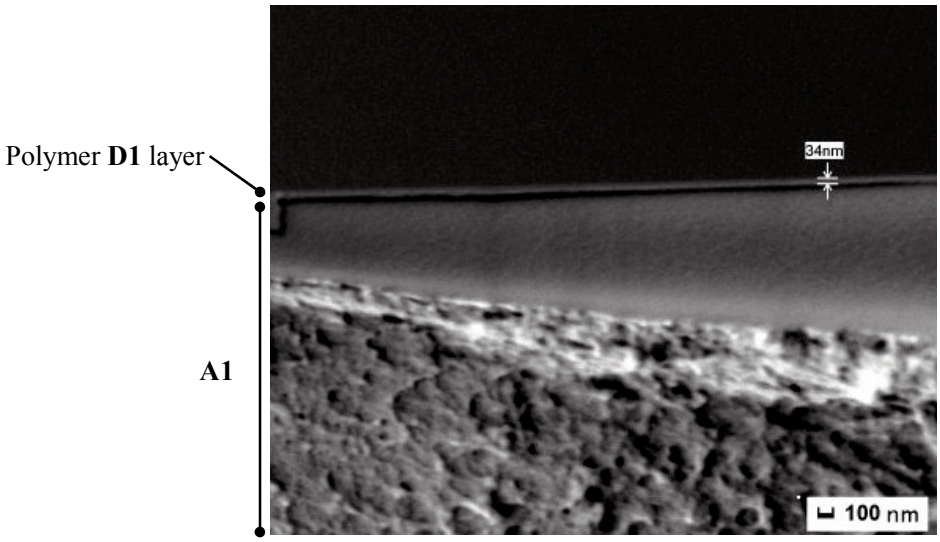

Figure S36 | FE-SEM image of polymer **D1** layer on **A1**.
Thickness of polymer **D1** layer is 34 nm.

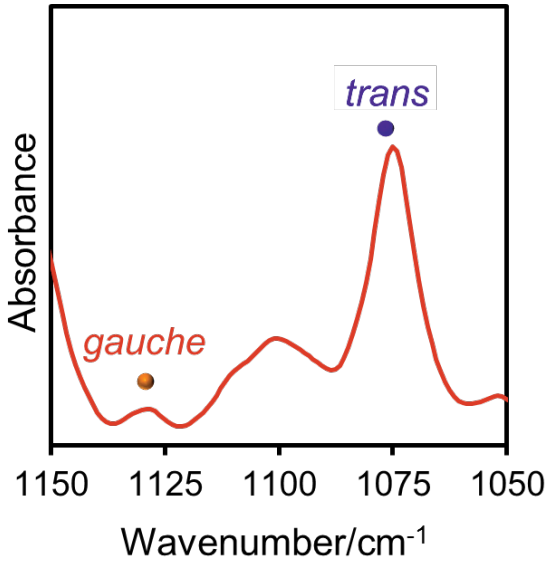

Figure S37 | FT-IR absorption spectrum associated with gauche and trans backbone conformations of **D1** on **A1**.

9. Characterization of the polymer dynamics of **D2** and **D3**.

DSC measurement and IR spectroscopy confirmed that **D2** and **D3** are low-flexibility rod-like polymers, with rigidities comparable to that of **D1**. The DSC measurements (Figs. S5 and S6) showed that they had very high T_g values (219 °C for **D2**, 264 °C for **D3**), which implied that the polymer chain had restricted mobility. The polymer-chain conformation was ascertained by FT-IR spectroscopy (Fig. S38). The peaks were assigned in the same way as for **D1**. The trans and gauche conformations of the poly(acrylamide) backbone were assigned based on the absorption bands at 1075 and 1130 cm^{-1}. **D2** and **D3** both showed a strong absorption peak at 1075 cm^{-1} and a smaller peak at 1130 cm^{-1}. Thus, we concluded that **D2** and **D3** were rod-like polymers with the main chain inhibiting the flexibility.

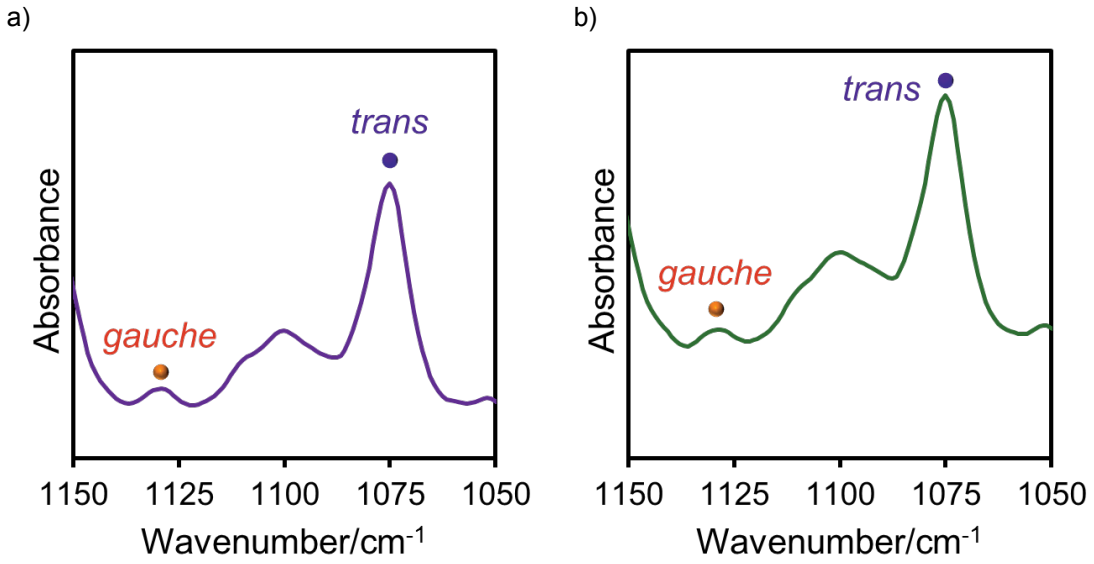

Figure S38 | FT-IR absorption spectrum associated with gauche and trans backbone conformations of a) **D2** and b) **D3** in chloroform.

10. Durability test of adhesion sample of **D1** and **A1**.

- Method

The soaking test was performed according to the following procedure. The **D1** and **A1** adhesion sample was soaked in boiling water for 5 h (Fig. S39a). Then, sample was dried at 80 °C for 1 h.

The long-term humidity and heat test was performed according to the following procedure. The **D1** and **A1** adhesion sample was exposed to constant temperature and humidity (85 °C, 85% RH) for 30 days (Fig. S39b). Then, sample was dried at 80 °C for 1 h.

After these treatments, the adhesion strength was estimated by a previously described method.

(a) (b)

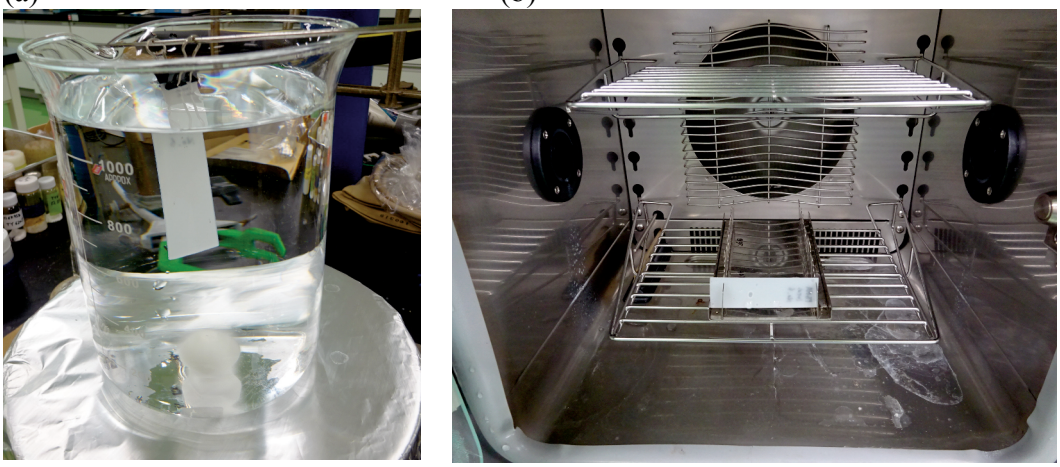

Figure S39 | Photograph of (a) the soaking test and (b) the long-term humidity and heat test.

11. Reference.

[1] Y. C. Kim, M. Jeon and S. Y. Kim, *Macromol. Rapid Commun.*, 2005, **26**, 1499.
[2] Y. Okamoto, M. Adachi, H. Shohi and H. Yuki, *Polym. J.*, 1981, **13**, 175.
[3] M. Matsumoto and T. Nishimura, *ACM Trans. Model. Comput. Simul.* 1998, **8**, 3.
[4] A. K. Rappé, C. J. Casewit, K. S. Colwell, W. A. Goddard III, W. M. Skiff and A. UFF, *J. Am. Chem. Soc.* 1992, **114**, 10024.
[5] K. C. Park, L. R. Dodd, K. Kevon and T. K. Kwei, *Macromolecules,* 1996, **29**, 7149.
[6] J. Wang, R. M. Wolf, J. W. Caldwell, P. A. Kollman and D. A. Case, *J. Comput. Chem.*, 2004, **25**, 1157.
[7] S. J. Plimpton, *J. Comp. Phys.,* 1995, **117**, 1.
[8] T. Darden, D. York and L. Pedersen, *J. Chem. Phys.,* 1993, **98**, 10089.
[9] S. A. Nosé, *J. Chem. Phys.,* 1984, **81**, 511.
[10] W. G. Hoover, *Phys. Rev. A: At., Mol., Opt. Phys.,* 1985, **31**, 1695.
[11] H. J. C. Berendsen, J. P. M. Postma, W. F. van Gunsteren, A. DiNola and J. R. Haak, *J. Chem. Phys.,* 1984, **81**, 3684.